Environmental and Experimental Botany 182 (2021) 104302

Contents lists available at ScienceDirect

Environmental and Experimental Botany

journal homepage: www.elsevier.com/locate/envexpbot

Sulphur and biothiol metabolism determine toxicity responses and fate of mercury in *Arabidopsis*

Juan Sobrino-Plata [a,1,2], Ángel Barón-Sola [a,1], Cristina Ortega-Villasante [a], Víctor Ortega-Campayo [a,3], Cesar González-Berrocal [a], Carlos Conesa-Quintana [a,3], Sandra Carrasco-Gil [b,4], María Muñoz-Pinilla [b], Javier Abadía [b], Ana Álvarez-Fernández [b], Luis E. Hernández [a,*]

[a] Laboratory of Plant Physiology, Department of Biology, Universidad Autónoma de Madrid, 28049 Madrid, Spain
[b] Department of Plant Nutrition, Aula Dei Experimental Station-CSIC, 50080 Zaragoza, Spain

ARTICLE INFO

Keywords:
Plant mercury stress
Plant S-assimilation
Biothiol dynamics
Xylem Hg-PC complexes

ABSTRACT

Mercury (Hg) is one of the most hazardous pollutants released by humans and is of global environmental concern. Mercury causes oxidative stress and strong cellular damages in plants, which can be attenuated by the biosynthesis of thiol-rich peptides (biothiols), including glutathione (GSH) and phytochelatins (PCs). We analysed Hg tolerance and speciation in five *Arabidopsis thaliana* genotypes, the wild-type Col-0, three knockdown γ-glutamylcysteine synthetase (γECS) mutants and a knockout PC synthase (PCS) mutant. Mercury-PC complexes were detected in roots by HPLC-ESI-TOFMS, with its abundance being limited in γECS mutants. Analysis of Hg-biothiol complexes in the xylem sap revealed that $HgPC_2$ occurs in wild-type Col-0 *Arabidopsis*, suggesting that Hg could be translocated associated with thiol-rich metabolites. Twenty genes involved in sulphur assimilation, GSH and PCs synthesis were differentially expressed in roots and shoots, implying a complex regulation, possibly involving post-translational mechanisms independent of GSH cellular levels. In summary, the present study describes the importance of biothiol metabolism and adequate GSH levels in Hg tolerance and identifies for the first time Hg-PC complexes in the xylem sap. This finding supports the notion that Hg-biothiol complexes could contribute to Hg mobilisation within plants.

1. Introduction

The often indiscriminate use of mercury (Hg) in several human activities, mostly related with chemical industries and gold-mining, and the use of ineffective waste removal practices has caused a progressive contamination of soils and groundwater worldwide (Li et al., 2008; Selin, 2009). Contamination by this hazardous metal needs to be tackled by using costly cleaning approaches that result in numerous environmental side effects (Chaney et al., 1997), whereas plant innate ability to take up metals can be exploited for soil phytoremediation (Krämer, 2005), in a sustainable low cost manner particularly appealing in Hg polluted areas (He et al., 2015; Marrugo-Negrete et al., 2016). However, this requires tolerant plants able to withstand cellular damages caused by toxic metal(loid)s (Rascio and Navari-Izzo, 2011). Among other mechanisms, Hg and other toxic metal(loid)s activate the rapid synthesis of thiol-rich peptides (biothiols) such as glutathione (GSH; γGlu-Cys-Gly) and phytochelatins (PC; $(\gamma Glu\text{-}Cys)_n$-Gly) where *n* has been reported as being as high as 11, but is generally in the range 2–5 (Cobbett, 2000; Serrano et al., 2015). Biothiols play a critical role in toxic metal tolerance by maintaining the intracellular redox balance and

* Corresponding author at: Laboratory of Plant Physiology, Department of Biology, Universidad Autónoma de Madrid, Campus de Cantoblanco, Darwin 2, 28049 Madrid, Spain.
E-mail address: luise.hernandez@uam.es (L.E. Hernández).
[1] Authors that contributed equally, and should be considered co-first authors
[2] Departamento de Sistemas y Recursos Naturales, Universidad Politécnica de Madrid, 28040 Madrid, Spain.
[3] Centre for Plant Biotechnology and Genomics (CBGP UPM-INIA), Universidad Politécnica de Madrid (UPM) & Instituto Nacional de Investigación y Tecnología Agraria y Alimentaria, Campus de Montegancedo, 28223 Pozuelo de Alarcón, Madrid, Spain
[4] Department of Agricultural Chemistry and Food Science, Universidad Autónoma de Madrid, 28049 Madrid, Spain.

https://doi.org/10.1016/j.envexpbot.2020.104302
Received 10 August 2020; Received in revised form 23 October 2020; Accepted 27 October 2020
Available online 4 November 2020

binding toxic metals to form less harmful chemical species (Hernández et al., 2015), which are translocated to vacuoles limiting the cytosolic concentration of free metal (Sharma et al., 2016). Sulphur assimilation and biothiol metabolism are thought to contribute to Hg tolerance and homeostasis (Carrasco-Gil et al., 2011), but there is still limited knowledge on regulatory mechanisms and how those metabolites mitigate Hg-induced stress.

The overall sulphur acquisition and assimilation pathway is highly conserved in the course of evolution starting with sulphate uptake by plant roots, and due to its large reduction energetic costs, it is mostly assimilated in leaves after xylem transport *via* different classes of sulphate transporters (SULT) (Gigolashvili and Kopriva, 2014). *Arabidopsis* has up to 14 sulphate transporter genes distributed in five groups (*AtSULTR1-5*), with Groups 1 and 2 being more related with S-assimilation (Kopriva, 2006). Once sulphate accumulates, assimilation starts with the synthesis of adenosine phosphosulphate (APS) by adenosine triphosphate sulphurylase (ATPS) from ATP in plastids (see pathway shown in Figs. 6 and 7). APS is reduced subsequently by APS reductase (APR), and then sulphite is reduced by sulphite reductase (SiR). The generated sulfhydryl ion binds to O-acetylserine in a step catalysed by OAS-thiol lyase (OAS-TL), synthesizing cysteine (Cys). This thiol-containing amino acid is then used by the enzyme γ-glutamylcysteine synthetase (γECS), which ligates Cys to glutamate (Glu), to generate γ-glutamylcysteine (γEC). Subsequently, glutathione synthetase (GSH-S) forms GSH from Gly and γEC (Kopriva et al., 2019).

In the present study we evaluate the response of different *Arabidopsis thaliana* genotypes with altered GSH levels under Hg stress, using three γECS mutant alleles *cad2-1*, *pad2-1* and *rax1-1*, which contain limited amounts of GSH relative to the wild type (Col-0) (Parisy et al., 2007), and a *cad1-3* PCS mutant unable to produce PCs (Cobbett, 2000). It is already known that Hg leads to specific stress alterations in biothiol metabolism in comparison with other toxic metals (Sobrino-Plata et al., 2009), but little information is available about its influence on sulphur metabolism. Hence, we analysed the changes in the transcriptional regulation of sulphate uptake and sulphur assimilation pathway under Hg stress. In addition, we determined Cys, Glu-Cys, GSH, and PCs accumulation in roots and shoots to assess plant biothiol distribution. Mercury is taken up by roots where it is strongly retained (Carrasco-Gil et al., 2011, 2013), and only a small portion is thought to be translocated to shoots *via* xylem, as occurs with other metal(loid)s (Khodamoradi et al., 2017); but it may be loaded to the xylem as chelated ions (Álvarez-Fernández et al., 2014). Here, we analysed xylem sap samples from different *Arabidopsis* genotypes for detection of Hg-biothiol complexes, and we show the presence of $HgPC_2$ complexes in *Arabidopsis* wild type, suggesting that Hg could be transported from the roots to the shoots not only as free ions but also as a biothiol chelated form.

2. Materials and methods

2.1. Plant material, growth conditions and treatments

A. thaliana genotypes used were the wild type Columbia 0 (Col-0), the *cad2-1*, *pad2-1* and *rax1-1* γECS mutants and the *cad1-3* PCS mutant. Seeds were surface-sterilized by agitation in a 15 % (v/v) NaClO solution for 10 min, followed by several rinses in distilled sterile water. Seeds were germinated on 0.6 % phytoagar and grown in an Araponics® hydroponic system (Araponics SA, Liège, Belgium). After 4 weeks of growth in a short-day light regime (8 h light / 16 h darkness) at 25 °C with a modified Hoagland nutrient solution (Tocquin et al., 2003), the nutrient solution was supplemented with 0 or 3 μM $HgCl_2$ and plants were grown for 72 h more. At harvest, shoots and roots were collected separately and stored at -80 °C until analysis.

2.2. Chlorophyll fluorescence measurements

Chlorophyll (Chl) fluorescence was measured at different light regimes to determine F_o, F_m, $F_{m'}$, F_t, $F_{o'}$, Φ_{PSII}, q_P and NPQ, according to (Maxwell and Johnson, 2000), using a FMS-2 Pulse Modulated Fluorimeter (Hansatech Instruments, Norfolk, UK). Plants were sequentially illuminated with 8000 μmol m^{-2} s^1 saturating pulses and 400 μmol m^{-2} s^1 actinic light.

2.3. Mercury and potassium tissue concentration

Organs were dried at 50 °C for 72 h, milled with mortar and pestle and 100 mg were placed in 4 mL glass vials, and mixed with 1 mL of digestion mixture (HNO_3:H_2O_2:H_2O, 0.6:0.4:1 v:v). After vials were securely enclosed with PTFE-stoppers, samples were digested using an autoclave (Presoclave-75 Selecta, Barcelona, Spain) at 120 °C and 1.5 atm for 30 min (Ortega-Villasante et al., 2007). Digests were filtered and diluted in Type I (MiliQ) water to 6 mL, prior to Hg and K concentrations determination using an ICP-MS NexION 300 Perkin-Elmer Sciex (San Jose, CA, USA) equipment.

2.4. Sequencing and alignment of γECS mutants

Genomic DNA was isolated from the shoots of Col-0, *cad2-1*, *pad2-1* and *rax1-1* plants using the DNA Extraction Kit Phytopure (GE Healthcare Life Sciences), and DNA concentration was measured in a NanoDrop® ND-1000 spectrophotometer (Thecnologies Inc., Wilmington, DE, USA). A 637 bp fragment of gene GSH1 (γ-glutamylcysteine synthetase, γ-ECS) was amplified by PCR using primers γECS01 F (CGTTCGGATTATTTCTTGGTGT) and γECS02R (GCGGTCCTTGTCAGTGTCTGT), and sequenced in an Applied Biosystems 3730/3730xl DNA Sequencer (Foster City, CA, USA). Sequences were revised using the Geneious Pro 5.5.3 software, and compared with GSH1 gene sequence (AT4G23100), and available literature (Supplementary Fig. S1).

2.5. RNA extraction and quantification

Total RNA from shoots and roots of *Arabidopsis* was isolated with TRI Reagent (Ambion, Austin, TX, USA), cleaned using in-column DNAse treatment with the RNeasy Mini Kit (Qiagen, Venlo, Netherlands) (Montero-Palmero et al., 2014), and quantified with a NanoDrop® ND-1000 spectrophotometer (Thecnologies Inc., Wilmington, DE, USA). RNA integrity was determined with an Agilent 2100 Bioanalyzer equipped with an RNA 6000 Nano LabChip Kit (Agilent Technologies, Santa Clara, CA, USA) using the RNA integrity number (RIN) algorithm of three independent biological replicates (Schroeder et al., 2006), which showed satisfactory RNA quality in all samples, particularly in those prepared from Hg-treated plants (Supplementary Fig. S2).

2.6. Quantitative reverse transcription polymerase chain reaction (qRT-PCR)

Quantitative reverse transcription (RT)-PCR was performed with RNA from *Arabidopsis* shoots and roots in two completely independent biological experiments (three RNA technical replicates each) to synthesize the complementary DNA strand. The RT reaction was performed with random hexamers, using the RETROscript® First Strand Synthesis Kit (Applied Biosystems-Life technologies, Carlsbad, CA, USA). Quantitative PCR was carried out with 50 ng single-stranded cDNA in a final volume of 20 μL, containing 10 μL of SYBR-Green Master Mix (Applied Biosystems-Life Technologies) and 250 nM forward and reverse specific primers (Life Technologies, Supplementary Table 1), using a Real-Time 7000SDS Termocycler (Applied Biosystems-Life Technologies), with denaturation at 95 °C for 10 min, 40 cycles of 15 s at 95 °C and 1 min annealing and extension at 60 °C. Gene expression was quantified by using the relative $2^{-\Delta\Delta Ct}$ method (Livak and Schmittgen, 2001), using the glyceraldehyde 3-phosphate dehydrogenase (GAPDH, AT1G13440) gene as internal reference, which showed steady expression under Hg

stress (Montero-Palmero et al., 2014).

2.7. Glutathione reductase in gel activity

GR enzymatic activities were determined *in gel* after separation of protein extracts using non-denaturing polyacrylamide electrophoresis (Sobrino-Plata et al., 2009). Protein loading was 20 and 10 μg for shoot and root samples, respectively. The staining solution was 250 mM Tris−HCl buffer, pH 7.5, supplemented with 0.2 mg mL^{-1} thizolyl blue tetrazolium bromide, 0.2 mg mL^{-1} 2,6-dichlorophenol indophenol, 0.5 mM NADPH and 3.5 mM GSSG.

2.8. Western-blot immunodetection

Immunodetection was performed by Western-blot after denaturing gel electrophoresis (Laemmli, 1970) and blotting onto a nitrocellulose membrane (BioTrace®NT Pall Corporation, East Hills, NY, USA), using a semi-dry procedure (Trans Blot® SD Semi-Dry Electrophoretic Transfer Cell; BioRad, Hercules, CA, USA). Membranes were incubated overnight at 4 °C with the primary antibodies (α-GR (AS06 181) that recognises both plastidial and cytoplasmic isoforms, dil. 1/5000; α−γECS (AS06 186), dil. 1/2500 (Agrisera, Vännäs, Sweden). After incubation with the anti-rabbit secondary antibody linked to horse radish peroxidase (HRP), proteins were detected using the LumiSensor Chemiluminescent HRP Kit (GenScript, Piscataway, NJ, USA), and images were taken with a ChemiDoc™ XRS + System (BioRad).

2.9. Oxidative stress visualisation by confocal laser scanning microscopy

Col-0 and mutant *Arabidopsis* were germinated for 15 days in Petri dishes filled with solid Murashige-Skoog nutrient solution (containing 1.0 % Phytagel, Sigma-Aldrich, San Luis, MI, USA). For oxidative stress staining, seedlings were transferred to a 24-well microtiter plate and immersed in 250 μL of 10 μM 2′,7′-dichlorofluorescein diacetate (H_2DCFDA) solution supplemented with 0 (control) or 3 μM Hg. After 30 min incubation in the darkness, seedlings were briefly counterstained with 25 μM propidium iodide (PI) to visualize cell death, and then samples were observed with a Leica TCS SP2 confocal microscope (Wetzlar, Germany) (Ortega-Villasante et al., 2007).

2.10. Xylem sap extraction and collection

Plants were collected and roots rinsed with distilled water, then excised at the caulinar (floral) stem above the rosette leaves, and the xylem sap was collected directly from the cut with a micropipette. To improve xylem sap exudation in Hg-stressed plants, roots were subjected to external pressure in a portable SKPM 1400 Scholander pressure chamber (SKYE Instruments Ltd., Powys, UK) by applying a 0.3 MPa constant pressure with compressed N_2 gas for less than 20 min. The first 10 μL were discarded to avoid cellular contamination, and the xylem sap collected (45 μL) was transferred to Eppendorf tubes containing 5 μL of acid mixture (10 % metaphosphoric acid, 1% formic acid and 10 mM EDTA), for preservation of biothiol and biothiol-Hg complexes. Samples were subsequently frozen at −80 °C and stored until analysis. Cross-contamination with cellular and phloem exudates was checked routinely by measuring L-malate dehydrogenase (c-MDH) activity (López-Millán et al., 2000) (see Extended Materials and Methods details in Supplementary online material).

2.11. Analysis of biothiols by HPLC-DAD

Biothiols in shoots and roots were analysed by HPLC-UV-diode array detector (DAD) (Sobrino-Plata et al., 2009). Extracts (100 μL) were injected in a Mediterranea SEA18 column (5 μm, 250 × 4.6 mm; Teknokroma, San Cugat del Vallés, Spain), using a 1200 HPLC system (Agilent, Santa Clara, CA, USA), and biothiols were detected after post-column derivatization with Ellman reagent. Quantification was carried out adding N-acetyl cysteine (N-AcCys; final concentration 250 μM) as internal standard prior to sample homogenization. See full methodology details in the Extended Materials and Methods of Supplementary material file.

2.12. Analysis of biothiols and ascorbate by HPLC-ESI-MS(TOF)

Ascorbate, biothiols and Hg–biothiol complexes were analysed by HPLC-electro spray ionisation (ESI)-time-of-flight mass spectrometry [MS(TOF)], using an HPLC system (Alliance 2795, Waters, Milford, MA, USA), equipped with a reverse-phase monolithic UPLC column (Mediterranea SEA18 3 μm 15 × 0.21 cm, Teknokroma), and coupled to a MS-TOF spectrometer (MicrOTOF, Bruker Daltonics, Bremen, Germany) equipped with an ESI source (Carrasco-Gil et al., 2011), with a mobile phase made with solvents A (0.1 % formic acid in miliQ water), and B (0.1 % formic acid in acetonitrile) (see Extended Materials and Methods details in Supplementary online material). After chromatographic separation, sample was directed with a flow rate of 200 μL min^{-1} to the ESI interface. The MS(TOF) operated in negative/positive ion mode at -500/4500 V endplate and spray tip voltages, respectively. The orifice voltage was set at 100 V and full scan data acquisition was carried out from *m/z* 50 to1000. The mass axis was calibrated externally using Li-formate adducts (10 mM LiOH, 0.2 % (v/v) formic acid and 50 % (v/v) 2-propanol). The HPLC-ESI-MS(TOF) system was controlled with MicrOTOF Control v.2.2 and HyStar v.3.2, and data were managed with Data Analysis v.3.4 (software packages from Bruker Daltonics). Ion chromatograms were extracted with a precision of 0.05 *m/z* units.

2.13. MS/MS for $HgPC_2$ complex analysis

For LC-MS^n (tandem MS spectra) measurements, the same HPLC system described above was used, including chromatographic column and analysis conditions, but the MS^n study was performed using a HCT Ultra high-capacity ion trap (Buker Daltonics). ESI conditions were as described previously and to establish the optimum MS^n conditions, standard solutions of $HgPC_2$ were tested. A volume of 20 μL of standard or xylem sap samples was injected into the LC system and MS^n analyses were controlled by HyStar v 3.2 software (Bruker Daltonics). MS^n experiments were conducted by selecting the high intensity peak mother ion (740.1 *m/z* for MS, and 536.1 *m/z* for MS^2) at the retention time of the compound chromatographic peak, and data were collected in total ion counting mode, acquiring the spectra in the range 100-1100 *m/z*.

2.14. Statistics

Statistical analysis was performed with SPSS for Windows (v. 19.0), using an ANOVA with Tukey test, with a factorial ANOVA to compare Hg concentration and chlorophyll fluorescence parameters between genotypes and Hg doses. Results shown are means of at least three replicates ± standard deviation, using $p < 0.05$ to detect statistically significant differences.

3. Results

Biothiol amounts in roots and shoots varied greatly depending on *Arabidopsis* genotypes according to the HPLC-DAD analysis (Fig. 1; Supplementary Table S2). Glutathione was present in all genotypes, but it was at remarkably low concentrations in the γECS mutants *cad2-1*, *pad2-1* and *rax1-1*, when compared with the levels of the wild type Col-0. Due to lack of phenotypic variations, all knock-down mutants were unequivocally identified by PCR amplification and sequence alignment (Supplementary Fig. S1), in agreement with the respective data reported by the labs that isolated those mutants, which express γECS allelic variants with limited catalytic enzymatic activity (Cobbett et al., 1998; Parisy et al., 2007; Ball et al., 2004). In the phytochelatin-defective

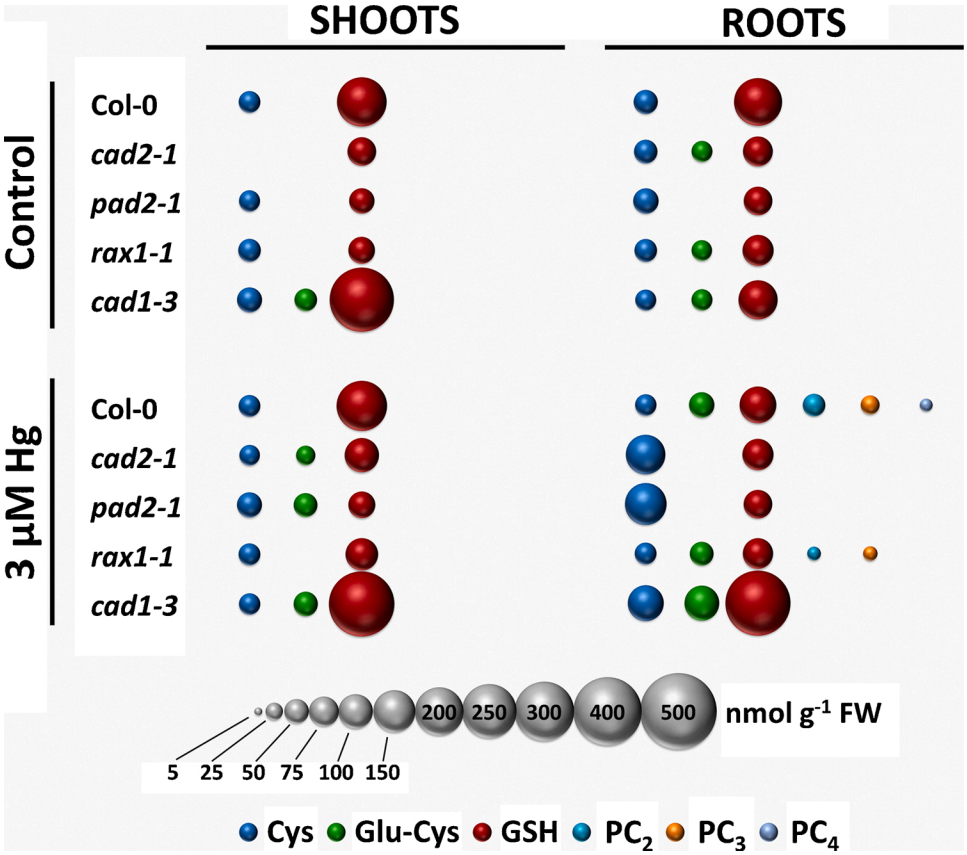

Fig. 1. Summary of HPLC-DAD analysis of biothiol concentrations in shoots and roots (in nmol·g^{-1} FW) in wild type (Col-0), *cad2-1*, *pad2-1*, *rax1-1* and *cad1-3 Arabidopsis thaliana* treated with 0 and 3 µM Hg for 72 h. Different biothiols are represented by spheres with different colours, with sphere diameters proportional to concentrations found. The concentration-to-volume scale is represented by the grey spheres at the bottom. Note that PC_2 were detected in roots of *cad2-1* and *pad2-1* treated with 3 µM Hg. but could not be quantified. For statistics and complete description of concentration values, please see Supplementary Table S2.

mutant *cad1-3*, the GSH concentration in shoots was approximately doubled that found in the wild type. In the presence of 3 µM Hg, PC_2 ($(\gamma Glu\text{-}Cys)_2$-Gly), PC_3 ($(\gamma Glu\text{-}Cys)_3$-Gly) and PC_4 ($(\gamma Glu\text{-}Cys)_4$-Gly) were found in Col-0 roots, whereas only PC_2 and PC_3 accumulated to lesser extent in *rax1-1* roots (Fig. 1; Supplementary Table S2). However, those PCs were barely detected in *cad2-1* and *pad2-1* mutants, and we were unable to quantify them. As expected, we could not detect PCs in *cad1-3* under Hg stress, even though GSH concentrations were the highest observed both in shoots and roots, twice the concentration found in *Arabidopsis* Col-0.

The decrease of GSH levels in *pad2-1*, *cad 2-1* and *rax1-1* and the inability to synthesize PCs in *cad1-3* were accompanied by significant changes in ascorbic acid (ASA), reduced (GSH) and oxidized glutathione (GSSG) concentrations, as measured by HPLC-ESI-MS(TOF) (Table 1). *Arabidopsis* mutants treated with 3 µM Hg had ASA concentrations in roots well above of values found in Col-0, which almost doubled in shoots. On the other hand, GSH concentrations followed the same pattern found using HPLC-DAD, with *pad2-1*, *cad2-1* and *rax1-1* having the lowest values both in roots and shoots, whereas the GSH concentration in *cad1-3* was 2-fold higher than Col-0. Exposure to 3 µM Hg led to general increases in GSH concentrations in shoots and roots of all mutant genotypes, particularly *cad1-3*. With respect to GSSG, concentrations were one order of magnitude lower than those of GSH, but they changed with a similar pattern. As a result, there were minimal changes in the relative content of GSSG irrespective of genotype and occurrence of Hg stress.

The marked changes in ASA and GSH/GSSG contents observed in response to Hg suggested possible alterations in the redox balance of mutant shoots and roots. We firstly analysed the concentrations of Hg in shoots and roots of *Arabidopsis*, which accumulated largely in roots (shoots Hg concentration was less than 1% of that found in roots; Fig. 2a). All γECS mutants had similar Hg levels in roots, which were approximately 50 % of the concentration found in Col-0 and *cad1-3* plants (Fig. 2a). However, there were not significant differences between genotypes but differed in comparison with the control (with $p < 0.001$; see Supplementary Table S3). In parallel, we determined photochemical parameters measured by chlorophyll *a* fluorescence, and observed that there were statistically differences between Hg treatments, *Arabidopsis* genotypes and the interaction of both variable factors (Supplementary Table S3). Non-photochemical quenching (NPQ) was severely impaired in γECS and PCS mutant genotypes both in control and 3 µM Hg-treated plants (Fig. 2b), confirming that limiting biothiols metabolism led to stress in leaves.

The specific inhibition of GR activity is a suitable biomarker of Hg toxicity (Sobrino-Plata et al., 2009), which dropped drastically in roots of GSH depleted mutants *cad2-1*, *pad2-1*, and *rax1-1*, whereas in Col-0 and *cad1-3* roots GR activity was ultimately higher (Fig. 3a). Despite such inhibition, the amount of GR protein did not change appreciably in roots even under Hg-stress independently of the genotype (Fig. 3b). Shoot GR activity only increased slightly in *pad2-1* and *cad1-3* without any substantial alteration in GR amount upon Hg stress (Fig. 3a). On the other hand, shoot γECS protein accumulation clearly diminished in γECS and *cad1-3* mutants under control conditions (40–50 % of that found in Col-0), pattern that was also observed under Hg stress in all genotypes (Fig. 3b). However, we could not detect changes in root γECS content among genotypes and Hg treatments, probably due to the low signal obtained by α-γECS immunodetection (high background; Fig. 3b). Redox imbalance associated with GSH depletion was confirmed by using confocal fluorescence microscopy, using H_2DCFDA for oxidative stress staining and IP counterstaining to visualize cell walls and cell death in 15-days old *Arabidopsis* seedlings. Under control conditions, some epidermal cells suffered oxidative stress (yellow arrowheads) probably caused by mechanical damage during manipulation of roots, more clearly observed in the GSH-deficient mutant *pad2-1* than in Col-0 (Fig. 3c), a symptom that also appeared in previous experiments with alfalfa seedlings (Ortega-Villasante et al., 2005, 2007). H_2DCFDA

Table 1
Concentration of ascorbic acid (ASA), reduced (GSH) and oxidized (GSSG) glutathione (in nmol g^{-1} FW) measured by HPLC-ESI-TOFMS, and glutathione redox ratio %GSSG [GSSG/(GSH + GSSG)] x 100] in wild type (Col-0), *cad2-1*, *pad2-1*, *rax1-1* and *cad1-3 Arabidopsis thaliana* treated with 0 and 3 μM Hg for 72 h. Different letters in the same column denote significant differences between treatments and genotypes at $p < 0.05$ (n = 4).

			ASA	GSH	GSSG	% GSSG
SHOOTS	Control	Col-0	4777.77^{a} ± 286.32	284.33^{a} ± 27.35	6.63^{a} ± 2.16	2.3
		cad2-1	5897.23^{a} ± 1719.75	37.12^{b} ± 14.31	1.22^{c} ± 0.31	3.2
		pad2-1	5413.97^{a} ± 840.92	13.49^{b} ± 3.62	0.87^{c} ± 0.37	6.0
		rax1-1	5472.31^{a} ± 663.86	55.41^{b} ± 3.55	3.66^{b} ± 0.56	6.2
		cad1-3	4595.73^{a} ± 291.22	312.09^{a} ± 32.47	6.10^{a} ± 1.18	1.9
	3 μM Hg	Col-0	6232.62^{a} ± 1890.08	281.16^{a} ± 43.41	9.25^{a} ± 1.33	3.2
		cad2-1	11718.71^{b} ± 1650.06	51.41^{b} ± 18.09	1.67^{c} ± 0.34	3.1
		pad2-1	11882.27^{b} ± 1126.86	21.08^{b} ± 5.80	1.37^{c} ± 0.82	6.1
		rax1-1	10728.59^{b} ± 1149.24	145.62^{c} ± 26.91	6.65^{a} ± 1.48	4.4
		cad1-3	10399.66^{b} ± 1413.69	406.59^{d} ± 32.64	12.83^{b} ± 1.50	3.1
ROOTS	Control	Col-0	1388.48^{a} ± 256.64	195.78^{a} ± 34.61	7.40^{a} ± 0.99	3.6
		cad2-1	1336.04^{a} ± 49.52	44.62^{cd} ± 10.28	1.99^{c} ± 0.61	4.3
		pad2-1	1357.04^{a} ± 260.35	14.09^{d} ± 1.65	0.93^{c} ± 0.33	6.2
		rax1-1	1302.52^{a} ± 25.00	55.38^{c} ± 3.49	3.71^{bc} ± 1.48	6.3
		cad1-3	1553.45^{b} ± 62.04	280.14^{ab} ± 5.50	11.19^{b} ± 0.88	3.8
	3 μM Hg	Col-0	1276.32^{a} ± 225.05	145.56^{a} ± 7.44	4.24^{a} ± 0.99	2.8
		cad2-1	1796.90^{b} ± 194.19	82.48^{c} ± 30.96	2.91^{ab} ± 0.23	3.4
		pad2-1	1707.96^{b} ± 125.50	63.68^{c} ± 11.38	2.92^{ab} ± 0.60	4.4
		rax1-1	1924.59^{b} ± 92.65	170.52^{d} ± 18.48	6.84^{a} ± 1.52	3.9
		cad1-3	1474.29^{ab} ± 129.65	513.82^{b} ± 46.85	25.03^{d} ± 0.34	4.6

oxidative stress increased in seedling roots exposed to 3 μM Hg for 30 min, at the time that IP staining of cell damage (pink arrowheads) occurred more clearly at the elongation and apical regions of *pad2-1* than in the wild-type, suggesting an earlier/stronger toxic effect of Hg in the γECS mutant despite individual variation between replicates (Fig. 3c). Similar pattern of Hg-induced damage occurred in *cad2-1* and *rax1-1*, while *cad3-1* was equal to the responses detected in Col-0 seedlings (data not shown). Finally, we confirmed the elevated susceptibility of γECS and PCS mutants to Hg by detecting a drastic drop in root K concentration (Supplementary Fig. S3), crucial macronutrient for plant cell osmotic balance, which was probably caused by loss of membrane integrity and ion leakage occurring upon abiotic stress (Demidchik et al., 2014).

Our preceding study established that the ability of plants to withstand Hg toxicity depends in part on the formation of Hg-PCs complexes, such as $HgPC_2$ ($Hg(\gamma GluCys)_2Gly$) and $HgPC_3$ ($Hg(\gamma GluCys)_3Gly$) (Carrasco-Gil et al., 2011). Full HPLC-ESI-MS(TOF) analysis of biothiol ligands and Hg-biothiol complexes (Hg-PCs) in shoots and roots of showed clear differences between all studied *Arabidopsis* genotypes (Fig. 4). In shoots, we could only detect free PC_2 ($[PC_2\text{-}H]^-$; *m/z* 538.1) and PC_3 ($[PC_3\text{-}H]^-$; *m/z* 770.2) ligands, whereas in roots there were oxidized variants of free PCs, such as ($[PC_3oxd\text{-}H]^-$; *m/z* 768.2), Hg-PC complexes like $HgPC_2$ ($[HgPC_2\text{-}H]^-$; *m/z* 738.1) and $HgPC_3$ ($[HgPC_3\text{-}H]^-$; *m/z* 970.1). The graphical table included in Fig. 4b shows the groups of free ligands, oxidised PCs and Hg-biothiol complexes, found in shoots and roots of all *Arabidopsis* genotypes. The results in *rax1-1* and *cad2-1* roots closely resembled those found for Col-0, where we detected $[HgPC_2\text{-}H]^-$ and $[HgPC_3\text{-}H]^-$, albeit with a rather weak signal (data not shown). On the other hand, in *pad2-1* we only found GSH ($[GSH+H]^+$; *m/z* 308.1) and GSSG ($[GSSG+H]^+$; *m/z* 613.3) in roots and shoots, which were better detected in positive mode, in addition to PC_2, that was just over the background signal. As expected, *cad1-3* did not accumulate free PCs or Hg-PCs complexes.

Recent studies indicated that toxic elements (Cd and As) are chelated with PCs in roots impeding translocation to shoots and potentially helping plants to attenuate stress, in a manner that metal(loid)-PCs complexes would accumulate in root vacuoles (Liu et al., 2010; Mendoza-Cózatl et al., 2008). However, to some extent metal(loid)s may travel to shoots bound to organic ligands such as PCs (Shi et al., 2019). To determine whether Hg had a similar behaviour, we studied the possible occurrence of biothiols and Hg-PCs complexes in xylem sap by HPLC-ESI-MS(TOF) using both positive and negative modes. Since Hg blocks water movement through plant vascular tissues, we used a Scholander pressure chamber to apply a pneumatic pressure to allow xylem sap to flow from the cut stem. Similarly, Hg almost blocked completely the xylem water flow in pea plants, whereas in Cd-treated plants root pressure sufficed to collect several μLs of xylem sap (Belimov et al., 2015). To prevent cross-contamination of phloem and broken cells fluids, particularly when relatively high pneumatic pressure was used, MDH activity was measured routinely in all xylem sap samples. Data shown in Supplementary Fig. S4 suggest that cross-contamination was negligible in three xylem sap samples obtained from *Arabidopsis* Col-0 treated with 3 μM Hg. The compounds GSH ($[GSH+H]^+$; *m/z* 308.1) and GSSG ($[GSSG+H]^+$; *m/z* 613.3) appeared in the xylem sap of all genotypes, albeit signals were lower in γECS mutants (data not shown). The characteristic PC_2 peak ($[PC_2+H]^+$; *m/z* 540.1) appeared in xylem sap of Col-0 and, at very low intensity, also in *rax1-1* (Fig. 5). This compound coeluted with another of *m/z* 538.1, which was tentatively identified as oxidized PC_2 (PC_2oxd). However, PC_2 or PC_2oxd were not detected in *cad2-1*, *pad2-1* and, as expected, PCS mutant *cad1-3*.

To confirm the nature of PC_2oxd we run in parallel a hydroponic experiment with Col-0 *Arabidopsis* treated with 10 μM Cd for 72 h. In this case, we got a better signal in MS(TOF) in negative mode with a *m/z* 536.1 ($[PC_2oxd\text{-}H]^-$) (Supplementary Fig. S5a); molecular ion that was subjected to tandem MS (-MS^2), and was compared with those obtained using PC_2 (*m/z* 538.13) and PC_2oxd (*m/z* 536.1) standards, which had characteristic daughter ions at *m/z* 254.1 and 128.0 (Supplementary Fig. S5c). Incidentally, we were unable to observe any Cd-PC complex, in spite of using ESI-MS(TOF) settings appropriate for detection of $CdPC_2$, as we obtained the characteristic peaks associated with the natural Cd isotopic distribution (major $[CdPC_2\text{-}H]^-$ peak at *m/z* 650.0) by direct injection of a Cd:PC_2 standard (Supplementary Fig. S5b).

In Col-0 xylem sap, along with to PC_2 and PC_2oxd we found only a compound with the characteristic Hg-isotopic fingerprint that could correspond to Hg-PCs complexes, which was tentatively assigned to $HgPC_2$, eluting separately from free biothiol ligands (Fig. 5a). The MS (TOF) spectrum (in positive mode) of the detected compound ($[HgPC_2+H]^+$; *m/z* 740.1) fitted well with theoretical data and also with a Hg:PC_2 standard mixture (1:1) (Fig. 5b). The identity of the *m/z* 740.1 ion peak of Col-0 xylem samples was confirmed using tandem MS/MS analysis. The same Hg:PC_2 standard mixture was used to set up analytical conditions, and the *m/z* 740.1 mother ion was selected and sent to the collision cell for fragmentation (MS^2). Several major daughter ions appeared with *m/z* 609.1, 536.1 and 508.1 both in the $HgPC_2$ standard and the Col-0 xylem sap (Fig. 5c). Some of these ions were tentatively identified by comparing with those detected in Hg-biothiol complexes analysis as follows: *m/z* 609.1 was assigned to $[HgPC_2\text{-}Glu]^+$; *m/z* 536.1 matched $[PC_2oxd\text{-}2\ H]^+$, and *m/z* 508.1 was assigned to $[HgGSH+H]^+$.

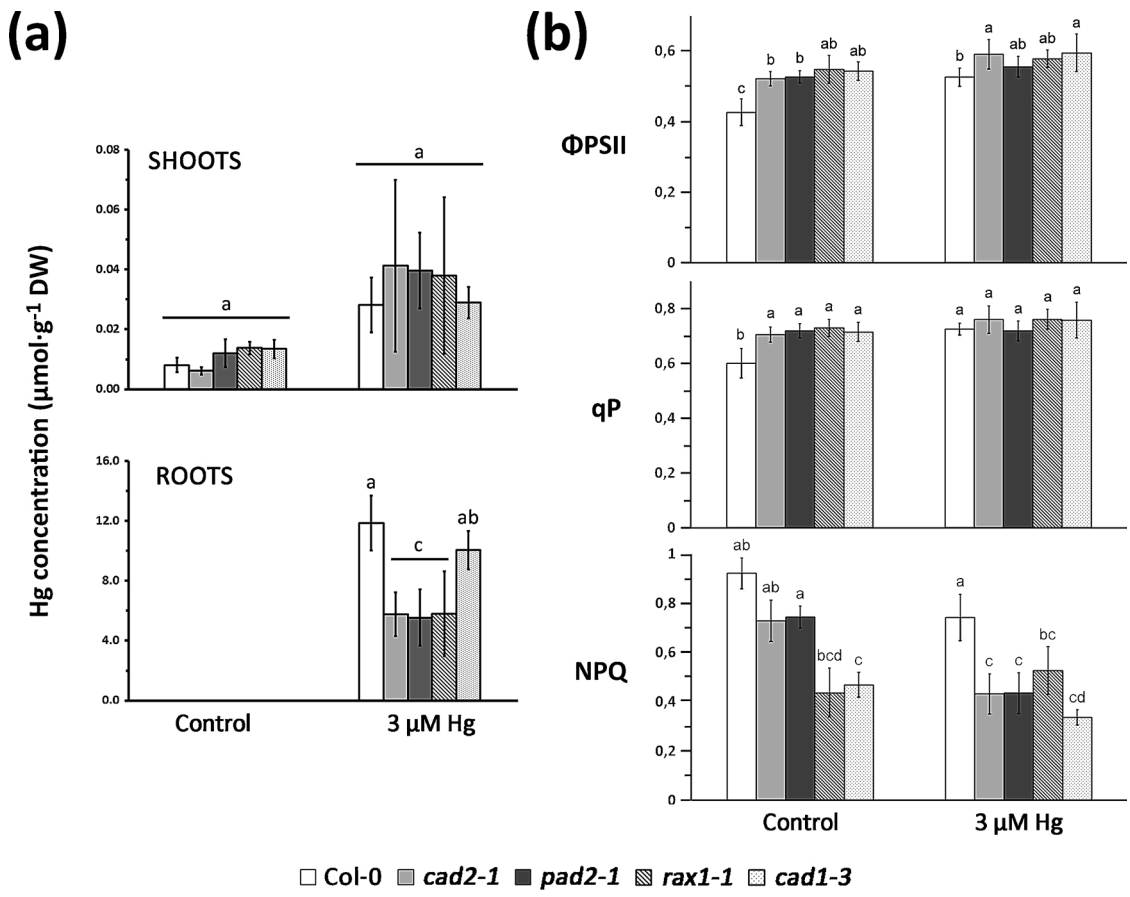

Fig. 2. **(a)** Mercury concentrations (µmol·g^{-1} DW) in roots and shoots, and (n = 4) **(b)** chlorophyll fluorescence parameters in wild type (Col-0), *cad2-1*, *pad2-1*, *rax1-1* and *cad1-3 Arabidopsis thaliana* treated with 0 and 3 µM Hg for 72 h: PSII efficiency (Φ_{PSII}), photochemical quenching (q_P) and non-photochemical quenching (NPQ) (n = 8). Different letters denote significant differences at $p < 0.05$.

Further identification of the *m/z* 536.1 ion, with the highest intensity peak, was obtained after a second fragmentation (MS^3) resulting in various ions. The MS^3 spectra of both the xylem sap and the standard mixture were also very similar, with a major *m/z* 507.1 daughter ion (possibly $[GSH\text{-}H]^+$), with a second *m/z* 489.1 ion also present in both samples (Fig. 5d). Therefore, we can assert that $HgPC_2$ complexes could be transferred from roots to shoots *via* xylem flux, process that did not occur in *rax1-1*, *cad2-1* and *cad1-3* mutants. Nevertheless, we could not determine to what extent Hg flows to shoots via xylem, since our ICP-MS analysis failed to detect Hg above background levels, probably due to the small volume of sample collected (10–50 µL).

In view of the relevant role that biothiol metabolism has in tolerance to and speciation of Hg in plants, we analysed the expression pattern of 20 genes involved in sulphur uptake, assimilation and incorporation to biothiols under Hg-stress (Gigolashvili and Kopriva, 2014). The expression pattern was organ-dependent, with some genes being over-expressed in the shoots of certain mutants treated with Hg (Fig. 6), whereas in the roots we only detected gene down-regulation under Hg stress (Fig. 7). Regarding transcription factors in shoots, *MYB28* was induced only in the γECS-mutants *cad2-1* and *pad2-1* under Hg exposure, whereas *MYB51* was suppressed in *rax1-1*. On the other hand, both *MYB28* and *MYB51* were down-regulated in roots under Hg-stress, especially in *rax1-1* and *cad1-3* mutants (Fig. 7). We also found significant down-regulation of SLIM1 in roots of all mutant *Arabidopsis* genotypes (Fig. 7; Supplementary Tables S4 and S5).

Among the genes involved in sulphur incorporation and assimilation in shoots, the sulphur transporter *SULTR1;2* had the highest over-expression in Hg-treated *cad2-1*, *rax1-1* and *cad1-3* plants, whereas a strong repression was observed in Col-0 (Fig. 6; Suppl. Table S4). A similar repression appeared in Col-0 for ATP sulphurylase (*ATPS3*) and APS reductase (*APR1* and *APR3*) (Fig. 6). On the other hand, *ATPS4* (only in *pad2-1*), *APR1*, *APR2* and *APR3* (only in *rax1-1*), were over-expressed in *pad2-1*, *rax1-1* and *cad1-3* plants treated with 3 µM Hg. With regard to GSH and PCs metabolism, we only observed a minor down-regulation under Hg stress, particularly significant for *cad2-1* and *pad2-1* O-acetylserine (thiol) lyase (*OASTLA* and *OASTLB*) genes. Interestingly, expression of the phytochelatin synthase genes *PCS1* and *PC2* decreased in leaves in Hg-treated plants, being particularly significant in *pad2-1*, *rax1-1* and *cad 1-3* (Fig. 6, Suppl. Table S4). Finally, in roots under Hg stress we only observed significant gene down-regulation, mostly in the mutant genotypes. Especially relevant was the down-regulation of sulphate transporters, including a remarkable decrease for *SULTR1;2* in *cad2-1*, *rax1-1* and *cad1-3* (Fig. 7). The expression of other sulphur transporters decreased, including that of *SULTR2;1* in *rax1-1* and *cad1-3*, and *SULTR3;5*, which was very intense in all Hg-exposed *Arabidopsis* genotypes. With regard to sulphur assimilation genes, the most consistent changes occurred in *cad1-3*, where *ATPS1*, *ATPS3*, *SiR*, *OASTLB*, *OASTLC*, *γECS*, *GSH-S*, *PCS1* and *PCS2* expression decreased in plants treated with 3 µM Hg (Fig. 7, Suppl. Table S5).

4. Discussion

Knock-down of γECS drastically decreased biothiol concentrations under control and Hg-stress conditions, particularly in the *cad2-1* and *pad2-1* mutants (Fig. 1), confirming previous results in these GSH-depleted genotypes (Parisy et al., 2007; Ball et al., 2004; Cobbett et al., 1998), and in *Arabidopsis* leaf discs and plants treated with similar

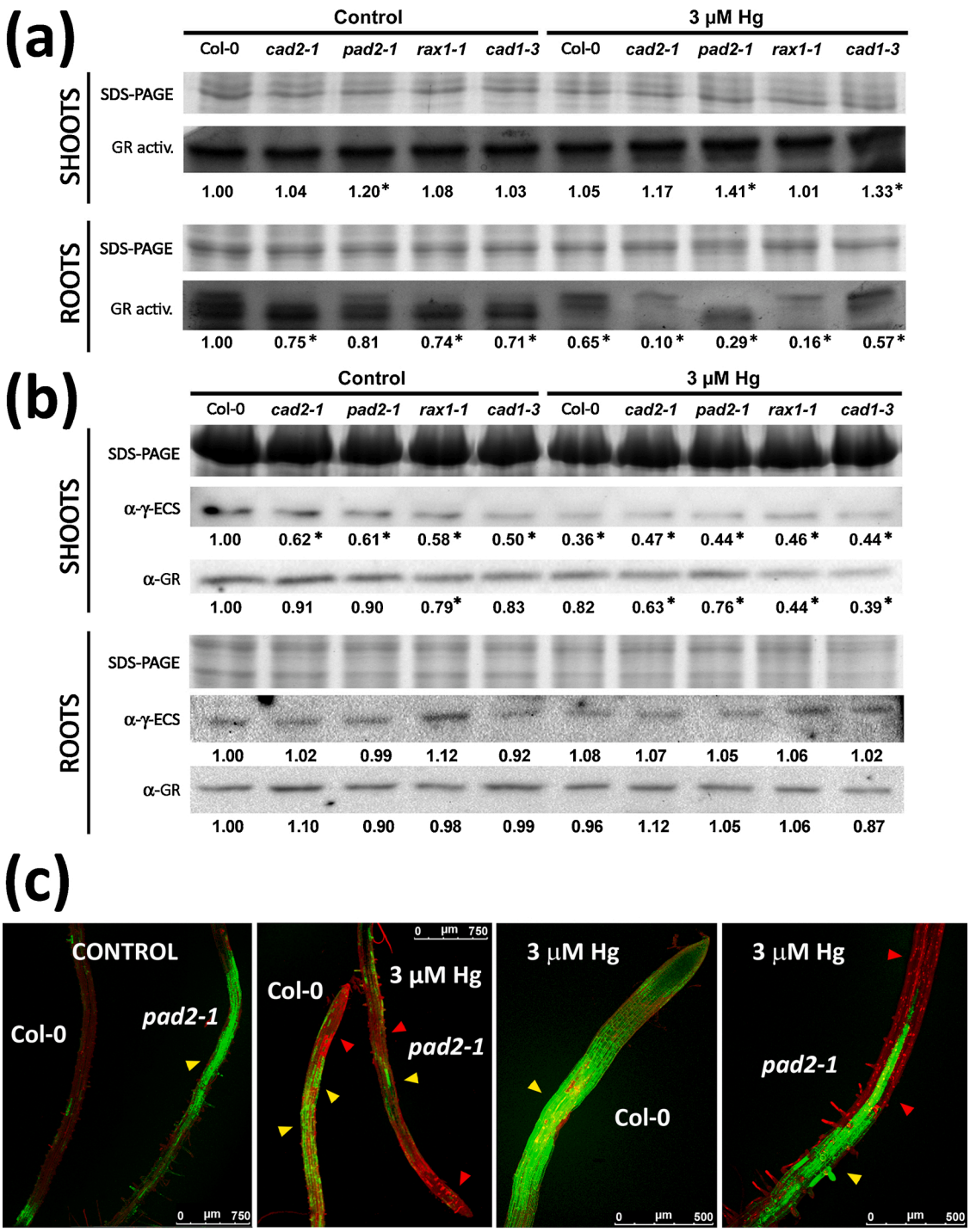

Fig. 3. **(a)** Glutathione reductase (GR) *in gel* activity, **(b)** γ−glutamylcysteine synthetase (γECS) and glutathione reductase (GR) immunodetection in wild type (Col-0), *cad2-1*, *pad2-1*, *rax1-1* and *cad1-3 Arabidopsis* treated with 0 (control) and 3 µM Hg for 72 h. Coomassie-blue staining was used to ensure sample equivalent protein loading. Numbers represent the fold-change relative to the control Col-0, with asterisks marking decreases and decreases ≥ 20 %. **(c)** Confocal fluorescence microscopy of *Arabidopsis* Col-0 and *pad2-1* seedling roots treated for 30 min with 0 (control) and 3 µM Hg (two specimens for comparison) to show oxidative stress (H_2DCFDA) induction (green, yellow arrowheads), counterstained with IP to visualise cell walls and detect necrotic cells (red; pink arrowheads).

doses of Hg and Cd (Sobrino-Plata et al., 2014a Sobrino-Plata et al., 2014a, 2014b). Interestingly, the mildly-affected knock-down *rax1-1* γECS mutant exposed to 3 µM Hg also accumulated PC_2 and PC_3 (but not PC_4) in roots, but to a lower extent than did wild-type plants as observed in Cd-treated plants (Sobrino-Plata et al., 2014b). We were unable to detect PCs in shoots, organs that accumulated much less Hg than roots (by two orders of magnitude), since a certain Hg concentration threshold may be required to trigger synthesis of PCs. In fact, numerous PCs appeared in Col-0 and *rax1-1* leaf discs subjected to direct infiltration with 3 and 30 µM Hg; behaviour that was accentuated at longer exposure times (48 h) when PC_2 and PC_3 also appeared in *cad2-1* (Sobrino-Plata et al., 2014a). On the other hand, the inability to synthesize PCs in *cad1-3* led to a significantly higher GSH accumulation when compared to Col-0 (Fig. 1, Table 1). Interestingly, this increase became larger under Hg stress, in agreement with our previous observations in *cad1-3* leaf discs infiltrated with 3 µM Hg for 24 h (Sobrino-Plata et al.,

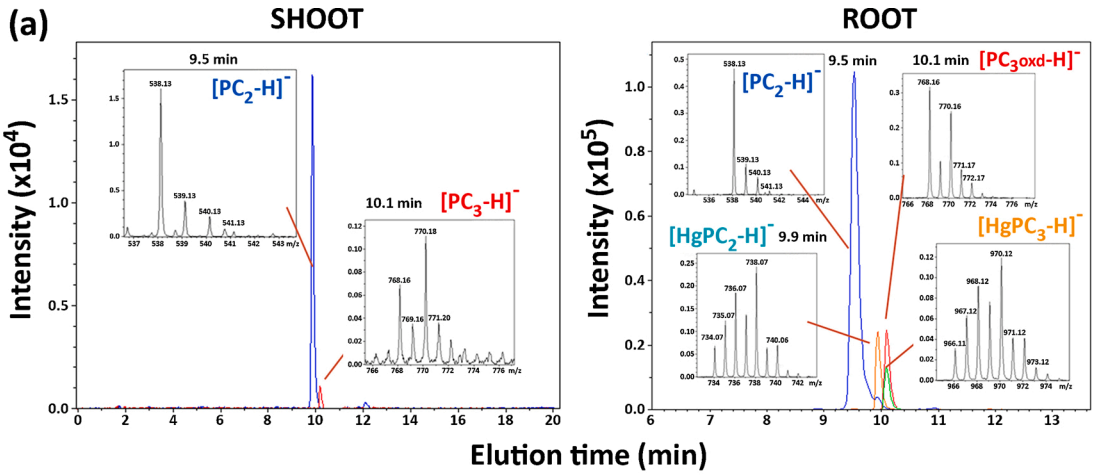

(b)

	Mol. ion	m/z	SHOOTS					ROOTS				
	Genotypes:		Col-0	*cad2-1*	*pad2-1*	*rax1-1*	*cad1-3*	Col-0	*cad2-1*	*pad2-1*	*rax1-1*	*cad1-3*
LIGANDS	$[GSH+H]^+$	308.1	■	■	■	■	■	■	■	■	■	■
	$[GSSG+H]^+$	613.3	■	■	■	■	■	■	■	■	■	■
	$[PC_2-H]^-$	538.1	■	■		■		■	■	■	■	
	$[PC_2oxd-H]^-$	536.1						■				
	$[PC_2+Na-H]^-$	560.1						■			■	
	$[PC_3-H]^-$	770.2	■			■		■	■		■	
	$[PC_3oxd-H]^-$	768.2	■			■		■	■		■	
	$[PC_3+Na-H]^-$	792.2						■				
COMPLEXES	$[HgPC_2-H]^-$	738.1						■	■	■	■	
	$[HgPC_2+Na-H]^-$	760.1						■			■	
	$[HgPC_3-H]^-$	970.1						■	■		■	
	$[HgPC_3+Na-H]^-$	992.1						■				

Fig. 4. PCs and Hg-PC complexes detected by HPLC-ESI-MS(TOF). **(a)** Examples of free PCs and Hg-PCs found in shoots and roots of Col-0 plants exposed to 3 μM Hg for 72 h. Chromatographs and characteristic MS spectra of several molecular ions are shown (in negative mode). **(b)** Summary table describing the different molecular ions of biothiol ligands and Hg-PC complexes detected in shoots and roots of all *Arabidopsis* genotypes treated with 3 μM Hg for 72 h. HPLC-ESI-MS(TOF) analysed in negative and positive modes, and major detected molecular ions (*m/z*) are shown.

2014a). It has been proposed recently that PCS functions as a transpeptidase important for GSH and conjugated GSH turnover, which may explain the high GSH levels found in *cad1-3* plants (Kühnlenz et al., 2015).

Depletion of GSH elicited a severe oxidative stress and enhanced cell death pattern with 3 μM Hg in *pad2-1*, resembling the patchy pattern that occurred under acute Hg stress in alfalfa seedlings that probably depends on the specific physiological status of each epidermal cell (Ortega-Villasante et al., 2007, 2005). Mercury stress also caused a marked inhibition of GR activity in the roots of γECS mutants in comparison with Col-0 and *cad1-3*, without any changes in enzyme amount. The mutant *cad1-3* lacked the ability to form Hg-PC complexes, but the Hg-induced damage was similar to that found in Col-0, possibly due to enhanced GSH levels in this mutant. Strong GR inhibition occurred in roots of *cad2-1*, *pad2-1* and *rax1-1* treated with 10 μM Hg for 72 h, which also suffered extensive alterations in membrane proteins (i.e., degradation of H^+-ATPase and strong inhibition of NADPH-oxidase; Sobrino-Plata et al., 2014b). Such alteration of membrane integrity would lead to ion leakage, which could explain low root K concentrations under Hg stress, particularly in γECS and PCS *Arabidopsis* mutants (Suppl. Fig. S3). Our results are thus comparable to the strong effects of Hg toxicity on K concentration observed in wheat (Sahu et al., 2012) and *Brassica juncea* (Wang et al., 2018) plants. Potassium is important for tolerance to various abiotic and biotic stresses, with a critical role in the osmotic and water balance of plant cells (Srivastava et al., 2020), which seem to be hampered by Hg particularly in GSH depleted *Arabidopsis* plants.

The GR inhibition appears to be triggered specifically by Hg over certain concentrations in *Medicago sativa* or *Silene vulgaris*, whereas other toxic elements usually lead to an enhanced activity (Sobrino-Plata et al., 2013, 2009), as can be used as a marker of Hg-stress. Paradoxically, besides the strong GR inhibition there were minor and non-consistent changes in the proportion of GSSG in the analysed *Arabidopsis* genotypes (Table 1), even though insufficient effective GR decreases the GSH/GSSG ratio (Müller-Schüssele et al., 2020). However, our results concurs with the minimal oxidation of homoglutathione (hGSH) (less than 15 %) found in extremely damaged alfalfa seedlings treated with 30 μM Hg (Ortega-Villasante et al., 2007). It is possible that even though GSH synthesis was compromised in γECS mutants, much severe and chronic cellular damage would be required to observe relevant GSH oxidation in roots. In addition, alternative pathways to maintain GSH cellular levels under Hg stress may operate: Recent

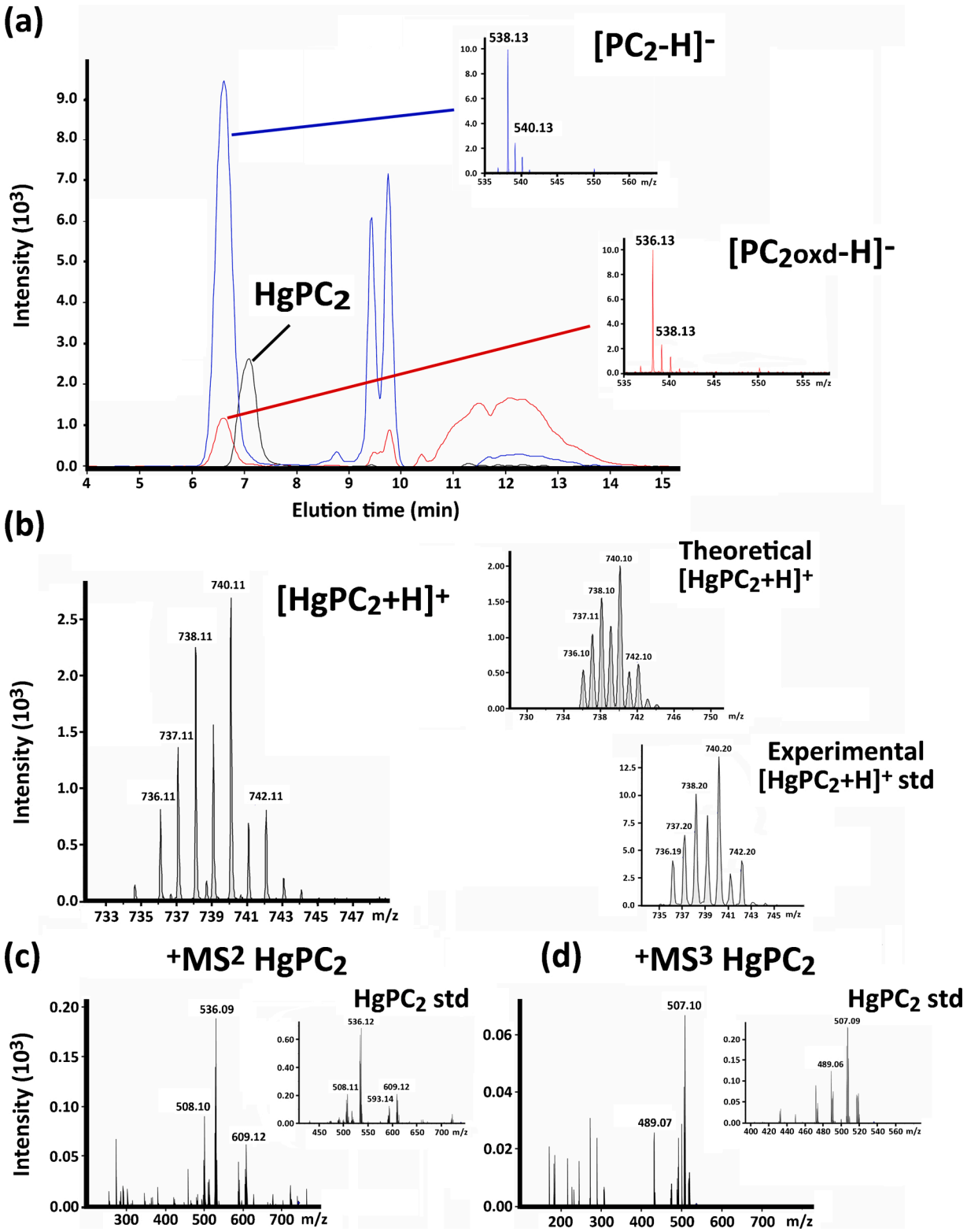

Fig. 5. HPLC-ESI-MS(TOF) analysis of PC and Hg–biothiol complexes in *Arabidopsis* Col-0 xylem sap. **(a)** Chromatographic profile of reduced PC_2, oxidized (PC_2oxd), and $HgPC_2$ detected in the xylem samples (in negative mode). **(b)** $[HgPC_2+H]^+$ molecular ion distribution (in *m/z*) compared with the theoretical one and a standard complex, prepared by mixing PC_2:$HgCl_2$ at 10:10 μM ratio (in positive mode). **(c)** and **(d)** MS^2 and MS^3 fragmentation profiles of $[HgPC_2+H]^+$, compared to those obtained using a standard PC_2:$HgCl_2$ mixture (insets), all in positive mode.

evidence suggest that methylglyoxal (MG), an ubiquitous toxic sub-product of carbon metabolism and lipid peroxidation that accumulates remarkably under plant abiotic stress, is detoxified with the sequential action of glyoxalase I (lactoylglutathione lyase) and glyoxalase II (hydroxyacylglutathione hydrolase) to generate GSH (Hoque et al., 2016). Incidentally, oxidative stress caused by Cd and Se in *Lepidium sativum* plants was associated with a strong accumulation of MG and other 2-oxoaldehydes (Gómez-Ojeda et al., 2013). Hence,

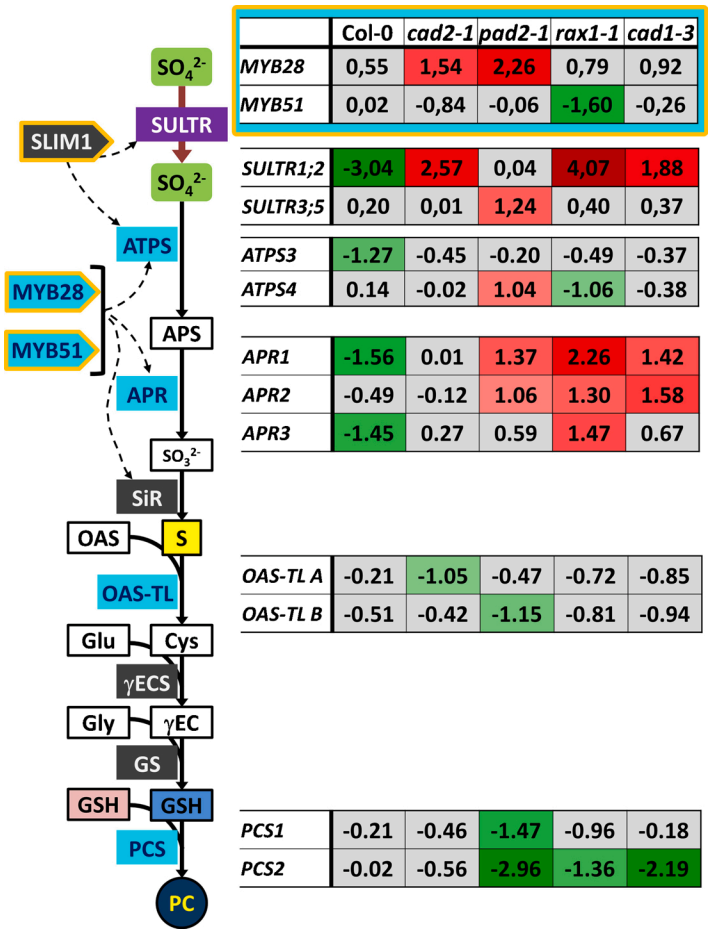

	Col-0	cad2-1	pad2-1	rax1-1	cad1-3
MYB28	0,55	1,54	2,26	0,79	0,92
MYB51	0,02	-0,84	-0,06	-1,60	-0,26
SULTR1;2	-3,04	2,57	0,04	4,07	1,88
SULTR3;5	0,20	0,01	1,24	0,40	0,37
ATPS3	-1.27	-0.45	-0.20	-0.49	-0.37
ATPS4	0.14	-0.02	1.04	-1.06	-0.38
APR1	-1.56	0.01	1.37	2.26	1.42
APR2	-0.49	-0.12	1.06	1.30	1.58
APR3	-1.45	0.27	0.59	1.47	0.67
OAS-TL A	-0.21	-1.05	-0.47	-0.72	-0.85
OAS-TL B	-0.51	-0.42	-1.15	-0.81	-0.94
PCS1	-0.21	-0.46	-1.47	-0.96	-0.18
PCS2	-0.02	-0.56	-2.96	-1.36	-2.19

Fig. 6. Shoot transcriptional qRT-PCR profile of selected genes related to sulphur metabolism, using Col-0, *cad2-1*, *pad2-1*, *rax1-1* and *cad1-3 Arabidopsis* treated with 0 or 3 μM Hg for 72 h. Values are presented as $\log_2$-fold change of Hg-treated plants relative to control plants of each genotype. Statistical differences with Col-0 (at $p < 0.05$) are represented as red and green boxes for over- and down-regulated genes, respectively. Grey boxes indicate no statistical differences. Data of genes encoding transcription factors ( ) are shown in the inset box ( ). Light blue boxes also highlight genes differentially expressed. See quantitative values and statistics in Supplementary Table S4.

elucidating whether this alternative stress response pathway operates also under Hg stress should be the matter of future experiments.

The poorer tolerance to Hg caused by limited GSH also led to alterations of chlorophyll fluorescence parameters, with a remarkable NPQ decrease (Fig. 2), in accordance with results obtained in *Arabidopsis* treated with Hg, Cd and Cu over 72 h (Maksymiec et al., 2007; Sobrino-Plata et al., 2014a). Alteration of GSH levels in γECS and PCS mutants decreased NPQ, observed even at control conditions, was also reported previously under metal stress in those *Arabidopsis* genotypes (Aranjuelo et al., 2014; Larsson et al., 2001). GSH plays a central role in chloroplast redox balance, keeping ASA and xanthophyll pools reduced at optimal levels to sustain NPQ under stress (Yin et al., 2010), which may be hampered in γECS mutants, or affected by excess GSH cellular concentration in *cad1-3*. Incidentally, transgenic tobacco plants engineered to overproduce GSH (2-fold increase than wild type plants) suffered stronger oxidative damage under high light stress in parallel with strong inhibition of photosynthesis (Creissen et al., 1999). On the other hand, the increase in ASA shoot concentrations under Hg stress was particularly intense in γECS mutant genotypes. Similar response was found in Cd-treated *cad2-1* mutants, where ASA concentration was higher than in wild-type plants (Jozefczak et al., 2015). In this respect, recent experiments showed that increases in ASA concentrations are a common response of plants to metal stress, especially in shoots where this antioxidant metabolite helps protecting the photosynthetic apparatus, which may be hampered by both the lack of GSH and the oxidative stress induced by Hg (Bielen et al., 2013). This damage could explain the diminution of the plastidial γECS content in shoots that appeared in *Arabidopsis* mutants even under control conditions, alteration that also appeared under Hg stress in all genotypes (Fig. 3b). The observed increase in ASA concentration under limited GSH concentration may be a general mechanism of ASA-GSH redox cycle acclimation, as was found in genetically engineered *Physcomitrella patens* with diminished functional GR and enhanced GSH oxidation subjected to high light stress (Müller-Schüssele et al., 2020).

Mercury is thought to bind strongly to cell walls of epidermal and vascular cells of the root, possibly bound to the Cys thiol residues of proteins, thus preventing translocation to shoots (Carrasco-Gil et al., 2011, 2013), as found in roots of different plant species (Carrasco-Gil et al., 2011; Sobrino-Plata et al., 2009, 2013; Sobrino-Plata et al., 2014b). Interestingly, γECS mutants roots had significant lower Hg concentration than Col-0, with no effects in shoots, whereas stronger Hg-induced damages appeared in the mutants. Similarly, metal accumulation in shoots did not change in Cd- and Hg-treated *cad2-1* plants (Li et al., 2006), in line with the view that cellular biothiol levels have little impact on overall plant metal distribution (Lee et al., 2003). On the other hand, it is known that transpiration is strongly impaired by Hg (Moreno et al., 2008), a toxic metal that drastically reduces metabolic-driven water conductance in roots (Lovisolo et al., 2008). Interestingly, short-term exposure of pea plants to 2 μM Hg led to drastic diminution of xylem flow (Belimov et al., 2015). This could also be related with the strong diminution of K concentration in roots, specifically in γECS *Arabidopsis* mutants, caused by 3 μM Hg; being K an important macronutrient for ionic and water plant homeostasis (Srivastava et al., 2020). Therefore, it is feasible that the strong Hg-stress in γECS mutants caused poorer water flow to shoot, which impelled us to use the Scholander pressure chamber to collect enough xylem sap. Ultimately, this toxic effect would also limit Hg and K uptake and translocation to the aerial part of Hg-exposed plants.

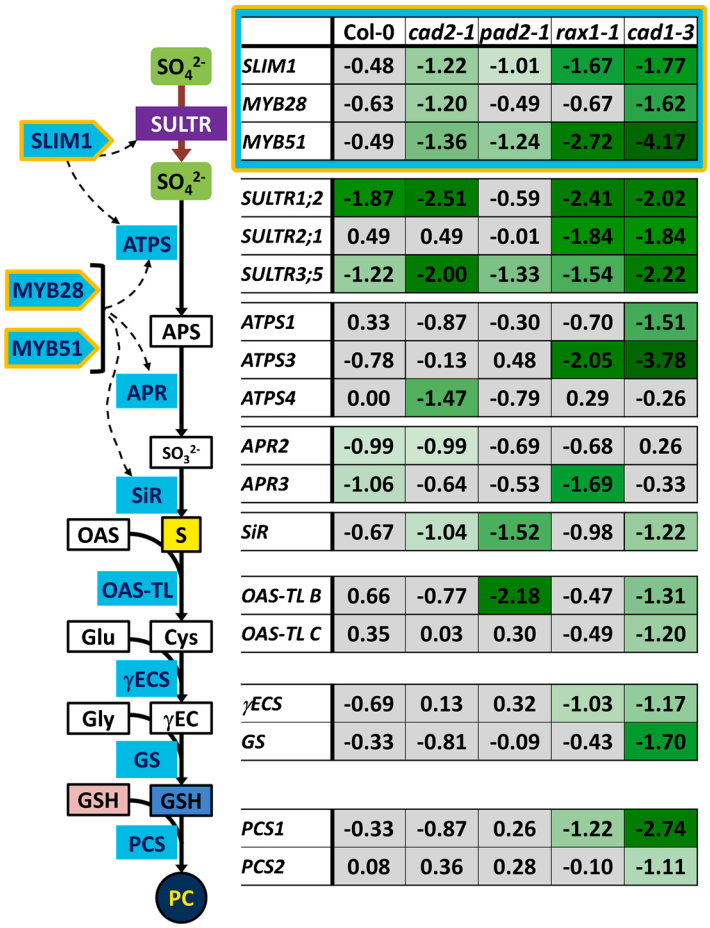

	Col-0	*cad2-1*	*pad2-1*	*rax1-1*	*cad1-3*
SLIM1	-0.48	-1.22	-1.01	-1.67	-1.77
MYB28	-0.63	-1.20	-0.49	-0.67	-1.62
MYB51	-0.49	-1.36	-1.24	-2.72	-4.17
SULTR1;2	-1.87	-2.51	-0.59	-2.41	-2.02
SULTR2;1	0.49	0.49	-0.01	-1.84	-1.84
SULTR3;5	-1.22	-2.00	-1.33	-1.54	-2.22
ATPS1	0.33	-0.87	-0.30	-0.70	-1.51
ATPS3	-0.78	-0.13	0.48	-2.05	-3.78
ATPS4	0.00	-1.47	-0.79	0.29	-0.26
APR2	-0.99	-0.99	-0.69	-0.68	0.26
APR3	-1.06	-0.64	-0.53	-1.69	-0.33
SiR	-0.67	-1.04	-1.52	-0.98	-1.22
OAS-TL B	0.66	-0.77	-2.18	-0.47	-1.31
OAS-TL C	0.35	0.03	0.30	-0.49	-1.20
γECS	-0.69	0.13	0.32	-1.03	-1.17
GS	-0.33	-0.81	-0.09	-0.43	-1.70
PCS1	-0.33	-0.87	0.26	-1.22	-2.74
PCS2	0.08	0.36	0.28	-0.10	-1.11

Fig. 7. Root transcriptional qRT-PCR profile of selected genes related to sulphur metabolism in Col-0, *cad2-1*, *pad2-1*, *rax1-1* and *cad1-3 Arabidopsis* treated with 0 or 3 μM Hg for 72 h. Values are presented as log_2-fold change of Hg-treated plants relative to control plants of each genotype. Statistically down-regulated genes when compared to Col-0 (at $p < 0.05$) are represented as green boxes, whereas grey boxes indicate no statistical difference. Data of genes encoding transcription factors (▰) are shown in the inset box (▣). Light blue boxes highlight genes differentially expressed. See quantitative values and statistics in Supplementary Table S5.

Xylem conforms, along with phloem, the major long-distance transport system for movement and distribution of water, ions and metals throughout the plant (Álvarez-Fernández et al., 2014). Cadmium transport by the xylem determines Cd accumulation in shoots, which depends on loading driven by metal transporters (Wu et al., 2015), while biothiols have been suggested as long distance carriers for Cd in the phloem of *Brassica napus* (Mendoza-Cózatl et al., 2008). The high stability of Hg-PC complexes found in plant roots could provide a basis for Hg long-distance transport, as it was suggested by the association of Hg with sulphur in stems and leaf veins of alfalfa plants exposed to Hg (Carrasco-Gil et al., 2013). HPLC-ESI-MS(TOF) analysis revealed for the first time that $[HgPC_2\text{-}H]^+$ indeed occurs in the xylem sap of Col-0 (Fig. 5), identity that was confirmed by MS^n analysis, with daughter molecular ions in the MS^2 and MS^3 spectra matching those of standards. We also detected free $[PC_2\text{-}H]^-$ and $[PC_2oxd\text{-}H]^-$ in xylem sap, confirming our preliminary findings in the xylem sap of Col-0 plants treated with 10 μM Cd for 72 h (Supplementary Fig. 2). Oxidised PC_2 was also found in the xylem sap of *Brassica napus* plants subjected to Cd (Mendoza-Cózatl et al., 2008) and *Arabidopsis* seedlings treated with As (Liu et al., 2010), but metal(loid)-PC complexes were not detected in those cases. Moreover, a very low concentration of As was found in xylem sap of the metallophyte castor bean, which was accompanied again with oxidised GSH and PC_2 (Ye et al., 2010), probably as a result of the oxidative stress and redox imbalance triggered by metal(loid)s. As(III)- and Cd-biothiols complexes may be less stable than those formed with Hg in our conditions, able to withstand even acidic extraction. Nevertheless, future research effort should be aimed to characterise the mechanism that controls xylem loading of Hg-PC complexes, which will probably require highly sensitive and spatially resolved analytical techniques.

Plants treated with metals experience alterations in sulphate uptake and assimilation (Na and Salt, 2011; Nocito et al., 2002, 2006), which prompted us to analyse the expression of twenty genes involved in the sulphur assimilatory pathway under Hg-stress. Our results revealed in all *A. thaliana* genotypes tested different responses to Hg in roots and shoots, indicating that both organs had independent stress responses as found with other metals (Jozefczak et al., 2014). In general, we observed a modest response of genes with fold-changes generally not larger than three (significant at $p < 0.05$), following the same pattern of recent transcriptomic analyses performed after short-term Hg treatments in *Medicago* (Montero-Palmero et al., 2014; Zhou et al., 2013), barley (Lopes et al., 2013), rice (Chen et al., 2014) and tomato (Hou et al., 2015).

With regard to sulphur metabolism regulation, several transcription factors have been reported to be overexpressed under S-starvation, such as the central hub SLIM1 regulator and several R2R3-MYBs, including MYB28 and MYB51 (Frerigmann and Gigolashvili, 2014). However, we only observed MYB28 upregulation in *cad2-1* and *pad2-1* shoots under Hg stress. Incidentally, a rice R2R3-MYB (OsARM1) has been found to be upregulated in stems and leaves upon As exposure (Wang et al., 2017), and several R2R3-MYBs control response to Cd-stress *via* ABA signalling (Zhang et al., 2019). However, we found marked MYB28, MYB51 and SLIM1 down-regulation in roots of Hg-stressed γECS and *cad1-3 Arabidopsis* mutants, which can likely explain the low expression of several sulphur assimilatory pathway genes. Little is known about how SLIM1 may operate under abiotic stress, which may undergo post-transcriptional redox imbalance regulation occurring in Hg-treated γECS mutants (Koprivova and Kopriva, 2014).

Sulphate uptake is a bottleneck in plant sulphur incorporation, through transporters that were upregulated under metal stress, such as

SULTR1;1 in roots of maize (Nocito et al., 2006) and *Arabidopsis* (Ferri et al., 2017). However, other members of the SULTR transporter gene family in sorghum and Chinese cabbage plantlets responded in different manner in leaves and roots under metal stresses (Akbudak et al., 2018; Shahbaz et al., 2014). We found that sulphate transporter *SULTR1;2* was up-regulated in shoots in *Arabidopsis* γECS and PCS mutants under Hg-stress, response was also found for *SULTR3;5* in roots of *Medicago* just after 6 h exposure to 3 μM Hg (Montero-Palmero et al., 2014). Conversely, *SULTR1;2* was down-regulated in shoots of Col-0 and roots of all *Arabidopsis* mutants, following the same pattern of *SULTR2;1* and *SULTR3;5* (Figs. 6 and 7), in agreement with the short-term down regulation of *SULTR3;3* in rice seedlings treated with 25 μM Hg for 3 h (Chen et al., 2014). Cadmium exposure and sulphate limitation revealed differences in the transcriptional control of three sulphate transporter (*SULTR1;2*) genes in *Brassica juncea* (Lancilli et al., 2014). Similarly, *SULTR1* and *SULTR2* expression decreased in roots and shoots of Cd-treated *Arabidopsis* at high Cd doses (over 40 μM) (Yamaguchi et al., 2016). Therefore, *SULTR* expression under metal stress changed depending on the plant organ, supplied metal and doses, implying a complex regulation and specific responses. Time-course experiments to monitor the metal induced expression of *SULTR1;2* showed that in roots it peaked a few hours after metal exposure but subsided subsequently (Jobe et al., 2012). It is feasible that the GSH depletion promoted *SULTR1;2* expression in shoots under Hg stress, where we observed significant redox alterations, whereas under acute cellular damage there might be a general transcriptional down-regulation in roots (Montero-Palmero et al., 2014).

APRs are key enzymes of sulphur assimilatory pathway, that produce sulphite from adenosine 5′ phosphosulphate (Kopriva, 2006), genes that were up-regulated in *Arabidopsis* γECS and PCS mutants shoots treated with Hg, in agreement with the overexpression found in short-term Hg-treated *Medicago* (Montero-Palmero et al., 2014). However, the rest of S-assimilatory pathway genes in shoots and roots of γECS and PCS mutants were modestly affected or down-regulated by Hg (Figs. 6,7). It must be emphasized that until now none of the transcriptomic analyses carried out in plants treated with Hg showed significant changes in gene expression of enzymes involved in Cys, γEC, GSH or PCs synthesis (Chen et al., 2014; Hou et al., 2015; Lopes et al., 2013; Montero-Palmero et al., 2014; Zhou et al., 2013). In consequence, despite the several significant changes in S-assimilatory gene expression, occurring mainly in GSH deprived plants, we cannot rule out that the process can be post-transcriptionally controlled. Several stress hormones and the redox cellular balance can contribute to altered enzymatic activities that modify biothiol pools (Kopriva et al., 2019); mechanisms that should be the matter of future research.

5. Conclusions

Depletion of GSH led to stronger Hg toxicity visualised by strong inhibition of GR activity, a poor accumulation of Hg-PC complexes and a limited translocation of $HgPC_2$ to shoots via xylem transport. Despite GR inhibition, the proportion of GSSG did not increase consistently with Hg-induced damage, which may imply the activation of alternative pathways to maintain GSH cellular pool, such as the methylglyoxal detoxification. Sulphur metabolism and accumulation of biothiols help withstanding Hg-induced oxidative stress, but the mechanisms of regulation remain to be characterised in detail. Although some responses at the transcriptional level were detected, we cannot rule out post-transcriptional regulation, which probably play a relevant role to procure sufficient biothiols to limit Hg induced damage. In this sense, transcriptional sulphur-assimilation regulation could be independent of GSH cellular levels, in spite of being an essential factor to maintain the cellular redox balance that was compromised by Hg.

Supplementary information file

Supplementary information contains extended Materials and Methods, alignment of γECS gene sequences of *Arabidopsis thaliana* genotypes used in our study, quality of RNA extracted from samples under Hg stress, concentration of K, MDH activity as a cytosolic contamination test in xylem sap, HPLC-ESI-TOFMS analysis of *Arabidopsis* treated with Cd, primers for qPCR analysis, concentration of biothiols in the different *Arabidopsis* genotypes exposed to Hg, factorial ANOVA data of photochemical parameters, and qRT-PCR expression values of selected genes of sulphur metabolism.

Authorship statement

All persons who meet authorship criteria are listed as authors, and on behalf of all authors the correspondence author certifies that they have participated sufficiently in the work to take public responsibility for the content, including participation in the concept, design, analysis, writing, or revision of the manuscript.

Furthermore, the correspondence author certifies that this material or similar material has not been and will not be submitted to or published in any other publication before its appearance in Environmental and Experimental Botany.

Authorship contributions

Conception and design of study: J. Sobrino-Plata, A. Barón-Sola, L.E. Hernández.

Acquisition of data: J. Sobrino-Plata, A. Barón-Sola, V. Ortega-Campayo, C. González-Berrocal, C. Conesa-Quintana, S. Carrasco-Gil, M. Muñoz-Pinilla, A. Álvarez-Fernández.

Analysis and/or interpretation of data: C. Ortega-Villasante, J. Abadía, A. Álvarez-Fernández, L.E. Hernández.

Drafting and editing the manuscript: J. Sobrino-Plata, A. Barón-Sola, C. Ortega-Villasante, J. Abadía, A. Álvarez-Fernández, L.E. Hernández.

Approval of the version of the manuscript to be published

Juan Sobrino-Plata, Ángel Barón-Sola, Cristina Ortega-Villasante, Víctor Ortega-Campayo, Cesar González-Berrocal, Carlos Conesa-Quintana, Sandra Carrasco-Gil, María Muñoz-Pinilla, Javier Abadía, Ana Álvarez-Fernández, Luis E. Hernández

All persons who have made substantial contributions to the work reported in the manuscript (e.g., technical help, general support), but who do not meet the criteria for authorship, are named in the Acknowledgements. This statement is signed by the corresponding author on behalf of all the authors.

Declaration of Competing Interest

The authors declare that they have no known competing financial interests or personal relationships that could have appeared to influence the work reported in this paper

Acknowledgments

Work supported by the Spanish State Research Agency (AEI) co-financed with the European Regional Development Fund (ERDF) (projects AGL2014-53771-R and AGL2017-87591-R to LEH and AGL2016-75226-R to AAF and JA; AEI/ERDF, UE). We thank Dr. M. Isabel Orús (Dept. Biology UAM, Madrid, Spain) for help in using the Scholander pressure chamber for obtaining xylem samples.

Appendix A. Supplementary data

Supplementary material related to this article can be found, in the online version, at doi:https://doi.org/10.1016/j.envexpbot.2020.104302.

References

Akbudak, M.A., Filiz, E., Kontbay, K., 2018. Genome-wide identification and cadmium induced expression profiling of sulfate transporter (*SULTR*) genes in sorghum (*Sorghum bicolor* L.). BioMetals. https://doi.org/10.1007/s10534-017-0071-5.

Álvarez-Fernández, A., Díaz-Benito, P., Abadía, A., López-Millán, A.F., Abadía, J., 2014. Metal species involved in long distance metal transport in plants. Front. Plant Sci. https://doi.org/10.3389/fpls.2014.00105.

Aranjuelo, I., Doustaly, F., Cela, J., Porcel, R., Müller, M., Aroca, R., Munné-Bosch, S., Bourguignon, J., 2014. Glutathione and transpiration as key factors conditioning oxidative stress in *Arabidopsis thaliana* exposed to uranium. Planta 239, 817–830. https://doi.org/10.1007/s00425-013-2014-x.

Ball, L., Accotto, G.P., Bechtold, U., Creissen, G., Funck, D., Jimenez, A., Kular, B., Leyland, N., Mejia-Carranza, J., Reynolds, H., Karpinski, S., Mullineaux, P.M., 2004. Evidence for a direct link between glutathione biosynthesis and stress defense gene expression in *Arabidopsis*. Plant Cell 16, 2448–2462. https://doi.org/10.1105/tpc.104.022608.

Belimov, A.A., Dodd, I.C., Safronova, V.I., Malkov, N.V., Davies, W.J., Tikhonovich, I.A., 2015. The cadmium-tolerant pea (*Pisum sativum* L.) mutant SGECdt is more sensitive to mercury: assessing plant water relations. J. Exp. Bot. 66, 2359–2369. https://doi.org/10.1093/jxb/eru536.

Bielen, A., Remans, T., Vangronsveld, J., Cuypers, A., 2013. The influence of metal stress on the availability and redox state of ascorbate, and possible interference with its cellular functions. Int. J. Mol. Sci. 14, 6382–6413. https://doi.org/10.3390/ijms14036382.

Carrasco-Gil, S., Alvarez-Fernández, A., Sobrino-Plata, J., Millán, R., Carpena-Ruiz, R.O., Leduc, D.L., Andrews, J.C., Abadía, J., Hernández, L.E., 2011. Complexation of Hg with phytochelatins is important for plant Hg tolerance. Plant Cell Environ. 34, 778–791. https://doi.org/10.1111/j.1365-3040.2011.02281.x.

Carrasco-Gil, S., Siebner, H., LeDuc, D.L., Webb, S.M., Millán, R., Andrews, J.C., Hernández, L.E., 2013. Mercury localization and speciation in plants grown hydroponically or in a natural environment. Environ. Sci. Technol. 47, 3082–3090.

Chaney, R.L., Malik, M., Li, Y.M., Brown, S.L., Brewer, E.P., Angle, J.S., Baker, A.J.M., 1997. Phytoremediation of soil metals. Curr. Opin. Biotechnol. https://doi.org/10.1016/S0958-1669(97)80004-3.

Chen, Y.A., Chi, W.C., Trinh, N.N., Huang, L.Y., Chen, Y.C., Cheng, K.T., Huang, T.L., Lin, C.Y., Huang, H.J., 2014. Transcriptome profiling and physiological studies reveal a major role for aromatic amino acids in mercury stress tolerance in rice seedlings. PLoS One 9, 1–11. https://doi.org/10.1371/journal.pone.0095163.

Cobbett, C.S., 2000. Phytochelatins and their roles in heavy metal detoxification. Plant Physiol. https://doi.org/10.1104/pp.123.3.825.

Cobbett, C.S., May, M.J., Howden, R., Rolls, B., 1998. The glutathione-deficient, cadmium-sensitive mutant, cad2-1, of *Arabidopsis thaliana* is deficient in γ-glutamylcysteine synthetase. Plant J. 16, 73–78. https://doi.org/10.1046/j.1365-313x.1998.00262.x.

Creissen, G., Firmin, J., Fryer, M., Kular, B., Leyland, N., Reynolds, H., Pastori, G., Wellburn, F., Baker, N., Wellburn, A., Mullineaux, P., 1999. Elevated glutathione biosynthetic capacity in the chloroplasts of transgenic tobacco plants paradoxically causes increased oxidative stress. Plant Cell 11, 1277–1291. https://doi.org/10.1105/tpc.11.7.1277.

Demidchik, V., Straltsova, D., Medvedev, S.S., Pozhvanov, G.A., Sokolik, A., Yurin, V., 2014. Stress-induced electrolyte leakage: the role of K^+-permeable channels and involvement in programmed cell death and metabolic adjustment. J. Exp. Bot. 65, 1259–1270. https://doi.org/10.1093/jxb/eru004.

Ferri, A., Lancilli, C., Maghrebi, M., Lucchini, G., Sacchi, G.A., Nocito, F.F., 2017. The sulfate supply maximizing *Arabidopsis* shoot growth is higher under long- than short-term exposure to cadmium. Front. Plant Sci. 8, 854. https://doi.org/10.3389/fpls.2017.00854.

Frerigmann, H., Gigolashvili, T., 2014. Update on the role of R2R3-MYBs in the regulation of glucosinolates upon sulfur deficiency. Front. Plant Sci. https://doi.org/10.3389/fpls.2014.00626.

Gigolashvili, T., Kopriva, S., 2014. Transporters in plant sulfur metabolism. Front. Plant Sci. https://doi.org/10.3389/fpls.2014.00442.

Gómez-Ojeda, A., Corrales-Escobosa, A.R., Wrobel, Kazimierz, Yanez-Barrientos, E., Wrobel, Katarzyna, 2013. Effect of Cd(II) and Se(IV) exposure on cellular distribution of both elements and concentration levels of glyoxal and methylglyoxal in *Lepidium sativum*. Metallomics 5, 1254–1261. https://doi.org/10.1039/c3mt00058c.

He, F., Gao, J., Pierce, E., Strong, P.J., Wang, H., Liang, L., 2015. In situ remediation technologies for mercury-contaminated soil. Environ. Sci. Pollut. Res. https://doi.org/10.1007/s11356-015-4316-y.

Hernández, L.E., Sobrino-Plata, J., Montero-Palmero, M.B., Carrasco-Gil, S., Flores-Cáceres, M.L., Ortega-Villasante, C., Escobar, C., 2015. Contribution of glutathione to the control of cellular redox homeostasis under toxic metal and metalloid stress. J. Exp. Bot. 66, 2901–2911. https://doi.org/10.1093/jxb/erv063.

Hoque, T.S., Hossain, M.A., Mostofa, M.G., Burritt, D.J., Fujita, M., Tran, L.S.P., 2016. Methylglyoxal: an emerging signaling molecule in plant abiotic stress responses and tolerance. Front. Plant Sci. 7, 1–11. https://doi.org/10.3389/fpls.2016.01341.

Hou, J., Liu, X., Wang, J., Zhao, S., Cui, B., 2015. Microarray-based analysis of gene expression in *Lycopersicon esculentum* seedling roots in response to cadmium, chromium, mercury, and lead. Environ. Sci. Technol. 49, 1834–1841. https://doi.org/10.1021/es504154y.

Jobe, T.O., Sung, D.Y., Akmakjian, G., Pham, A., Komives, E.A., Mendoza-Cózatl, D.G., Schroeder, J.I., 2012. Feedback inhibition by thiols outranks glutathione depletion: A luciferase-based screen reveals glutathione-deficient γ-ECS and glutathione synthetase mutants impaired in cadmium-induced sulfate assimilation. Plant J. 70, 783–795. https://doi.org/10.1111/j.1365-313X.2012.04924.x.

Jozefczak, M., Keunen, E., Schat, H., Bliek, M., Hernández, L.E., Carleer, R., Remans, T., Bohler, S., Vangronsveld, J., Cuypers, A., 2014. Differential response of*Arabidopsis* leaves and roots to cadmium: Glutathione-related chelating capacity vs antioxidant capacity. Plant Physiol. Biochem. 83, 1–9. https://doi.org/10.1016/j.plaphy.2014.07.001.

Jozefczak, M., Bohler, S., Schat, H., Horemans, N., Guisez, Y., Remans, T., Vangronsveld, J., Cuypers, A., 2015. Both the concentration and redox state of glutathione and ascorbate influence the sensitivity of *Arabidopsis* to cadmium. Ann. Bot. https://doi.org/10.1093/aob/mcv075.

Khodamoradi, K., Khoshgoftarmanesh, A.H., Maibody, S.A.M.M., 2017. Root uptake and xylem transport of cadmium in wheat and triticale as affected by exogenous amino acids. Crop Pasture Sci. https://doi.org/10.1071/CP17061.

Kopriva, S., 2006. Regulation of sulfate assimilation in *Arabidopsis* and beyond. Ann. Bot. https://doi.org/10.1093/aob/mcl006.

Kopriva, S., Malagoli, M., Takahashi, H., 2019. Sulfur nutrition: Impacts on plant development, metabolism, and stress responses. J. Exp. Bot. https://doi.org/10.1093/jxb/erz319.

Koprivova, A., Kopriva, S., 2014. Molecular mechanisms of regulation of sulfate assimilation: first steps on a long road. Front. Plant Sci. https://doi.org/10.3389/fpls.2014.00589.

Krämer, U., 2005. Phytoremediation: novel approaches to cleaning up polluted soils. Curr. Opin. Biotechnol. https://doi.org/10.1016/j.copbio.2005.02.006.

Kühnlenz, T., Westphal, L., Schmidt, H., Scheel, D., Clemens, S., 2015. Expression of *Caenorhabditis elegans* PCS in the AtPCS1-deficient *Arabidopsis thaliana cad1-3* mutant separates the metal tolerance and non-host resistance functions of phytochelatin synthases. Plant Cell Environ. https://doi.org/10.1111/pce.12534.

Laemmli, U.K., 1970. Cleavage of structural proteins during the assembly of the head of bacteriophage T4. Nature. https://doi.org/10.1038/227680a0.

Lancilli, C., Giacomini, B., Lucchini, G., Davidian, J.C., Cocucci, M., Sacchi, G.A., Nocito, F.F., 2014. Cadmium exposure and sulfate limitation reveal differences in the transcriptional control of three sulfate transporter (*Sultr1;2*) genes in *Brassica juncea*. BMC Plant Biol. https://doi.org/10.1186/1471-2229-14-132.

Larsson, E.H., Bornman, J.F., Asp, H., 2001. Physiological effects of cadmium and UV-B radiation in phytochelatin-deficient *Arabidopsis thaliana*, *cad1-3*. Aust. J. Plant Physiol. 28, 505–512. https://doi.org/10.1071/PP01067.

Lee, S., Petros, D., Moon, J.S., Ko, T.S., Goldsbrough, P.B., Korban, S.S., 2003. Higher levels of ectopic expression of *Arabidopsis* phytochelatin synthase do not lead to increased cadmium tolerance and accumulation. Plant Physiol. Biochem. 41, 903–910. https://doi.org/10.1016/S0981-9428(03)00140-2.

Li, Y., Dankher, O.P., Carreira, L., Smith, A.P., Meagher, R.B., 2006. The shoot-specific expression of γ-glutamylcysteine synthetase directs the long-distance transport of thiol-peptides to roots conferring tolerance to mercury and arsenic. Plant Physiol. 141, 288–298. https://doi.org/10.1104/pp.105.074815.levels.

Li, P., Feng, X., Shang, L., Qiu, G., Meng, B., Liang, P., Zhang, H., 2008. Mercury pollution from artisanal mercury mining in Tongren, Guizhou. China. Appl. Geochem. https://doi.org/10.1016/j.apgeochem.2008.04.020.

Liu, W.J., Wood, B.A., Raab, A., McGrath, S.P., Zhao, F.J., Feldmann, J., 2010. Complexation of arsenite with phytochelatins reduces arsenite efflux and translocation from roots to shoots in *Arabidopsis*. Plant Physiol. https://doi.org/10.1104/pp.109.150862.

Livak, K.J., Schmittgen, T.D., 2001. Analysis of relative gene expression data using real-time quantitative PCR and the $2^{-\Delta\Delta CT}$ method. Methods. https://doi.org/10.1006/meth.2001.1262.

Lopes, M.S., Iglesia-Turiño, S., Cabrera-Bosquet, L., Serret, M.D., Bort, J., Febrero, A., Araus, J.L., 2013. Molecular and physiological mechanisms associated with root exposure to mercury in barley. Metallomics. https://doi.org/10.1039/c3mt00084b.

López-Millán, A.F., Morales, F., Abadía, A., Abadía, J., 2000. Effects of iron deficiency on the composition of the leaf apoplastic fluid and xylem sap in sugar beet. Implications for iron and carbon transport. Plant Physiol. 124, 873–884. https://doi.org/10.1104/pp.124.2.873.

Lovisolo, C., Tramontini, S., Flexas, J., Schubert, A., 2008. Mercurial inhibition of root hydraulic conductance in *Vitis* spp. Rootstocks under water stress. Environ. Exp. Bot. https://doi.org/10.1016/j.envexpbot.2007.11.005.

Maksymiec, W., Wójcik, M., Krupa, Z., 2007. Variation in oxidative stress and photochemical activity in *Arabidopsis thaliana* leaves subjected to cadmium and excess copper in the presence or absence of jasmonate and ascorbate. Chemosphere 66, 421–427. https://doi.org/10.1016/j.chemosphere.2006.06.025.

Marrugo-Negrete, J., Marrugo-Madrid, S., Pinedo-Hernández, J., Durango-Hernández, J., Díez, S., 2016. Screening of native plant species for phytoremediation potential at a Hg-contaminated mining site. Sci. Total Environ. 542, 809–816. https://doi.org/10.1016/j.scitotenv.2015.10.117.

Maxwell, K., Johnson, G.N., 2000. Chlorophyll fluorescence - A practical guide. J. Exp. Bot. https://doi.org/10.1093/jxb/51.345.659.

Mendoza-Cózatl, D.G., Butko, E., Springer, F., Torpey, J.W., Komives, E.A., Kehr, J., Schroeder, J.I., 2008. Identification of high levels of phytochelatins, glutathione and cadmium in the phloem sap of *Brassica napus*. A role for thiol-peptides in the long-

distance transport of cadmium and the effect of cadmium on iron translocation. Plant J. 54, 249–259. https://doi.org/10.1111/j.1365-313X.2008.03410.x.
Montero-Palmero, M.B., Martín-Barranco, A., Escobar, C., Hernández, L.E., 2014. Early transcriptional responses to mercury: a role for ethylene in mercury-induced stress. New Phytol. 201, 116–130. https://doi.org/10.1111/nph.12486.
Moreno, F.N., Anderson, C.W.N., Stewart, R.B., Robinson, B.H., 2008. Phytofiltration of mercury-contaminated water: volatilisation and plant-accumulation aspects. Environ. Exp. Bot. https://doi.org/10.1016/j.envexpbot.2007.07.007.
Müller-Schüssele, S.J., Wang, R., Gütle, D.D., Romer, J., Rodriguez-Franco, M., Scholz, M., Buchert, F., Lüth, V.M., Kopriva, S., Dörmann, P., Schwarzländer, M., Reski, R., Hippler, M., Meyer, A.J., 2020. Chloroplasts require glutathione reductase to balance reactive oxygen species and maintain efficient photosynthesis. Plant J. 103, 1140–1154. https://doi.org/10.1111/tpj.14791.
Na, G.N., Salt, D.E., 2011. The role of sulfur assimilation and sulfur-containing compounds in trace element homeostasis in plants. Environ. Exp. Bot. 72, 18–25. https://doi.org/10.1016/j.envexpbot.2010.04.004.
Nocito, F.F., Pirovano, L., Cocucci, M., Sacchi, G.A., 2002. Cadmium-induced sulfate uptake in maize roots. Plant Physiol. https://doi.org/10.1104/pp.002659.
Nocito, F.F., Lancilli, C., Crema, B., Fourcroy, P., Davidian, J.-C., Sacchi, G.A., 2006. Heavy metal stress and sulfate uptake in maize roots. Plant Physiol. https://doi.org/10.1104/pp.105.076240.
Ortega-Villasante, C., Rellán-Álvarez, R., Del Campo, F.F., Carpena-Ruiz, R.O., Hernández, L.E., 2005. Cellular damage induced by cadmium and mercury in *Medicago sativa*. J. Exp. Bot. 56, 2239–2251. https://doi.org/10.1093/jxb/eri223.
Ortega-Villasante, C., Hernández, L.E., Rellán-Alvarez, R., Del Campo, F.F., Carpena-Ruiz, R.O., 2007. Rapid alteration of cellular redox homeostasis upon exposure to cadmium and mercury in alfalfa seedlings. New Phytol. 176, 96–107. https://doi.org/10.1111/j.1469-8137.2007.02162.x.
Parisy, V., Poinssot, B., Owsianowski, L., Buchala, A., Glazebrook, J., Mauch, F., 2007. Identification of PAD2 as a γ-glutamylcysteine synthetase highlights the importance of glutathione in disease resistance of *Arabidopsis*. Plant J. https://doi.org/10.1111/j.1365-313X.2006.02938.x.
Rascio, N., Navari-Izzo, F., 2011. Heavy metal hyperaccumulating plants: How and why do they do it? And what makes them so interesting? Plant Sci. 180, 169–181. https://doi.org/10.1016/j.plantsci.2010.08.016.
Sahu, G.K., Upadhyay, S., Sahoo, B.B., 2012. Mercury induced phytotoxicity and oxidative stress in wheat (*Triticum aestivum* L.) plants. Physiol. Mol. Biol. Plants 18, 21–31. https://doi.org/10.1007/s12298-011-0090-6.
Schroeder, A., Mueller, O., Stocker, S., Salowsky, R., Leiber, M., Gassmann, M., Lightfoot, S., Menzel, W., Granzow, M., Ragg, T., 2006. The RIN: an RNA integrity number for assigning integrity values to RNA measurements. BMC Mol. Biol. https://doi.org/10.1186/1471-2199-7-3.
Selin, N.E., 2009. Global biogeochemical cycling of mercury: a review. Annu. Rev. Environ. Resour. 34, 43–63. https://doi.org/10.1146/annurev.environ.051308.084314.
Serrano, N., Díaz-Cruz, J.M., Ariño, C., Esteban, M., 2015. Recent contributions to the study of phytochelatins with an analytical approach. TrAC - Trends Anal. Chem. https://doi.org/10.1016/j.trac.2015.04.031.
Shahbaz, M., Stuiver, C.E.E., Posthumus, F.S., Parmar, S., Hawkesford, M.J., De Kok, L.J., 2014. Copper toxicity in Chinese cabbage is not influenced by plant sulphur status, but affects sulphur metabolism-related gene expression and the suggested regulatory metabolites. Plant Biol. https://doi.org/10.1111/plb.12019.
Sharma, S.S., Dietz, K.J., Mimura, T., 2016. Vacuolar compartmentalization as indispensable component of heavy metal detoxification in plants. Plant Cell Environ. https://doi.org/10.1111/pce.12706.
Shi, W., Zhang, Y., Chen, S., Polle, A., Rennenberg, H., Luo, Z., Bin, 2019. Physiological and molecular mechanisms of heavy metal accumulation in nonmycorrhizal versus mycorrhizal plants. Plant Cell Environ. https://doi.org/10.1111/pce.13471.
Sobrino-Plata, J., Meyssen, D., Cuypers, A., Escobar, C., Hernández, L.E., 2014a. Glutathione is a key antioxidant metabolite to cope with mercury and cadmium stress. Plant Soil 377, 369–381. https://doi.org/10.1007/s11104-013-2006-4.
Sobrino-Plata, J., Ortega-Villasante, C., Laura Flores-Cáceres, M., Escobar, C., Del Campo, F.F., Hernández, L.E., 2009. Differential alterations of antioxidant defenses as bioindicators of mercury and cadmium toxicity in alfalfa. Chemosphere 77, 946–954. https://doi.org/10.1016/j.chemosphere.2009.08.007.
Sobrino-Plata, J., Carrasco-Gil, S., Abadía, J., Escobar, C., Álvarez-Fernández, A., Hernández, L.E., 2014b. The role of glutathione in mercury tolerance resembles its function under cadmium stress in *Arabidopsis*. Metallomics 6, 356–366. https://doi.org/10.1039/C3MT00329A.
Sobrino-Plata, J., Herrero, J., Carrasco-Gil, S., Pérez-Sanz, A., Lobo, C., Escobar, C., Millán, R., Hernández, L.E., 2013. Specific stress responses to cadmium, arsenic and mercury appear in the metallophyte *Silene vulgaris* when grown hydroponically. RSC Adv. 3, 4736–4744. https://doi.org/10.1039/C3RA40357B.
Srivastava, A.K., Shankar, A., Chandran, A.K.N., Sharma, M., Jung, K.H., Suprasanna, P., Pandey, G.K., Foyer, C., 2020. Emerging concepts of potassium homeostasis in plants. J. Exp. Bot. 71, 608–619. https://doi.org/10.1093/jxb/erz458.
Tocquin, P., Corbesier, L., Havelange, A., Pieltain, A., Kurtem, E., Bernier, G., Perilleux, C., 2003. A novel high efficiency, low maintenance, hydroponic system for synchronous growth and flowering of *Arabidopsis thaliana*. BMC Plant Biol. https://doi.org/10.1186/1471-2229-3-2.
Wang, F.Z., Chen, M.X., Yu, L.J., Xie, L.J., Yuan, L.B., Qi, H., Xiao, M., Guo, W., Chen, Z., Yi, K., Zhang, J., Qiu, R., Shu, W., Xiao, S., Chen, Q.F., 2017. OsARM1, an R2R3 MYB Transcription factor, is involved in regulation of the response to arsenic stress in rice. Front. Plant Sci. https://doi.org/10.3389/fpls.2017.01868.
Wang, J., Anderson, C.W.N., Xing, Y., Fan, Y., Xia, J., Shaheen, S.M., Rinklebe, J., Feng, X., 2018. Thiosulphate-induced phytoextraction of mercury in *Brassica juncea*: spectroscopic investigations to define a mechanism for Hg uptake. Environ. Pollut. 242, 986–993. https://doi.org/10.1016/j.envpol.2018.07.065.
Wu, Z., Zhao, X., Sun, X., Tan, Q., Tang, Y., Nie, Z., Hu, C., 2015. Xylem transport and gene expression play decisive roles in cadmium accumulation in shoots of two oilseed rape cultivars (*Brassica napus*). Chemosphere. https://doi.org/10.1016/j.chemosphere.2014.09.099.
Yamaguchi, C., Takimoto, Y., Ohkama-Ohtsu, N., Hokura, A., Shinano, T., Nakamura, T., Suyama, A., Maruyama-Nakashita, A., 2016. Effects of cadmium treatment on the uptake and translocation of sulfate in *Arabidopsis thaliana*. Plant Cell Physiol. https://doi.org/10.1093/pcp/pcw156.
Ye, W.L., Wood, B.A., Stroud, J.L., Andralojc, P.J., Raab, A., McGrath, S.P., Feldmann, J., Zhao, F.J., 2010. Arsenic speciation in phloem and xylem exudates of castor bean. Plant Physiol. https://doi.org/10.1104/pp.110.163261.
Yin, Y., Li, S., Liao, W., Lu, Q., Wen, X., Lu, C., 2010. Photosystem II photochemistry, photoinhibition, and the xanthophyll cycle in heat-stressed rice leaves. J. Plant Physiol. https://doi.org/10.1016/j.jplph.2009.12.021.
Zhang, P., Wang, R., Ju, Q., Li, W., Tran, L.S.P., Xu, J., 2019. The R2R3-MYB transcription factor MYB49 regulates cadmium accumulation. Plant Physiol. https://doi.org/10.1104/pp.18.01380.
Zhou, Z.S., Yang, S.N., Li, H., Zhu, C.C., Liu, Z.P., Yang, Z.M., 2013. Molecular dissection of mercury-responsive transcriptome and sense/antisense genes in *Medicago truncatula*. J. Hazard. Mater. 252–253, 123–131. https://doi.org/10.1016/j.jhazmat.2013.02.011.